Multilayered Space-Time Coding for MIMO Systems

May Gomaa

A Thesis

in

The Department

of

Electrical and Computer Engineering

Presented in Partial Fulfillment of the Requirements

for the Degree of Master of Applied Science

Concordia University

Montreal, Quebec, Canada

December 2007

Your file Votre référence
ISBN: 978-0-494-40882-7
Our file Notre référence
ISBN: 978-0-494-40882-7

Abstract

Multilayered Space-Time Coding for MIMO Systems

May Gomaa

Merging layered space-time coding (LST), which provides high data rate transmission with space-time block coding (STBC) provides transmit diversity and improved performance to wireless communication systems. This architecture is known as multilayered space-time coding (MLSTC). In this thesis we propose a decreased complexity minimum mean squared error (MMSE) detector based on the sorted QR decomposition (SQRD), intended for the detection of multi-user STBC systems. The proposed decoder has been proven to enhance the overall performance of the MLSTC architecture. It offers a lower computational complexity than that offered by conventional detectors such as group interference cancellation (GIC) detectors. In addition, the number of receive antennas required to perform detection is smaller than that required by the GIC detector. Further, in order for all groups, which can be viewed as individual users, to benefit from a similar performance, unequal power allocation strategy will be employed to the system. We also concatenate OFDM to the MLSTC scheme in order to combat a frequency selective channel. We then extend this scheme to space-frequency-time (SFT) codes in order to extract the maximum frequency diversity available from the channel. In this thesis, we also propose a new transceiver architecture for multiple-input multiple-output (MIMO) systems. The proposed scheme borrows ideas from the MLSTC and threaded space-time coding (TSTC) schemes in an effort to maximize the diversity order while maintaining a low complexity detection. Specifically, the proposed scheme has a structure similar to that of the MLSTC while it employs a spatial interleaver (SI) in front of the MLSTC encoder. We analyze the proposed scheme where we derive an upper bound on the bit error rate and derive the diversity-multiplexing gain trade-off curve. We present several examples through which we demonstrate the superiority of the proposed scheme over existing schemes.

Dedicated to my dearest mother, sister, and family...

Acknowledgments

I would like to express my high appreciation to my academic supervisor Dr. Ali Ghrayeb for his support, constructive guidance and valuable discussions throughout my thesis research. Without his continuous encouragement and inspiring suggestions I would not have completed my thesis.

I would like to thank the committee members Dr. Y. R. Shayan, Dr. R. Raut, and Dr. Y. Zeng. Their comments have helped make the presentation of this thesis more coherent.

I extend many thanks to my colleagues, Xiang Nian Zeng, Mohamed El-fituri, Pooyan Haghighat, Jeyadeepan Jeganathan, Ghaleb Al Habian, and Hui Wan for their support and friendship.

Most notably, I would like to thank my family, to whom this dissertation is dedicated, for their never-ending, unconditional, loving support, and for the constant encouragement during my studies.

Contents

List of Figures

List of Tables

Chapter 1

Introduction

The telecommunication industry has shifted towards high data rate applications with 3G and 4G services. This leads to an increasing demand for high data rate communication services. This increase challenges the rate, speed and reliability provided by the wireless communication system. With limited accessible radio spectrum, higher data rates can be achieved solely by designing more efficient signaling techniques. Multiple-input multiple-output (MIMO) systems, which are composed with multiple element array antennas at both ends of the wireless link are a good solution to the new challenges faced in the telecommunication industry. MIMO systems demonstrate a remarkable increase in capacity when compared to single antenna systems [1], [2].

There are two major challenges that exist in wireless communication. The first phenomenon is fading in the wireless channel. Fading is defined as the time variation of the received signal power strength caused by changes in the channel. These changes in the channel can be caused by small-scale effects such as multipath fading as well as large-scale effects such as path loss through distance decrease and shadowing by obstacles. The second challenge is that significant interference exists in the wireless channel between different users.

Traditional design of wireless systems has focused on increasing the reliability of the wireless channel. Recent focus has shifted towards increasing the data rate or spectral efficiency. More interesting will be the design of a wireless system that can provide a valuable trade-off between reliability and spectral efficiency.

1.1 MIMO Capacity

The background for studying performance restrictions in communication is information theory. The fundamental measure of performance is the capacity of a channel, which is defined

as the maximum rate of communication for which subjectively small error probability can be realized. Shannon [3] was the first to bring light to information theory in 1948. Shannon's findings illustrated the limits of reliable communication [3]. MIMO systems have shown remarkable capacity increase over single antenna systems. The capacity limit of MIMO systems underline the possible spectral efficiency of MIMO channels, which increases approximately linearly with the number of antennas without sacrificing expensive bandwidth. This potential has lead to numerous designs of MIMO architectures [2], [4], [5], [6], [7]. Unlike traditional systems where the reduction of the effect of multipath propagation takes place, MIMO systems capture the advantages of space and time propagation characteristics. For the limited spectrum of mobile and cellular communications, MIMO systems are an excellent cost-effective candidate. The results of information theory demonstrate that the capacity of MIMO system increases linearly with $min(N_r, N_t)$, where N_r and N_t are the number of receive and transmit antennas, respectively [8], [1]. Conversely, for single-input single-output (SISO) channels, the capacity increases logarithmically with signal-to-noise ratio (SNR). Therefore, a considerable capacity enhancement can be realized by MIMO systems without the need to add power to the system and without expanding the bandwidth.

Figure 1.1 depicts a MIMO system. The signals are transmitted by multiple transmit antennas through the wireless channel. The signal is received at the receiver by multiple receive antennas and detectors are used to recover the message.

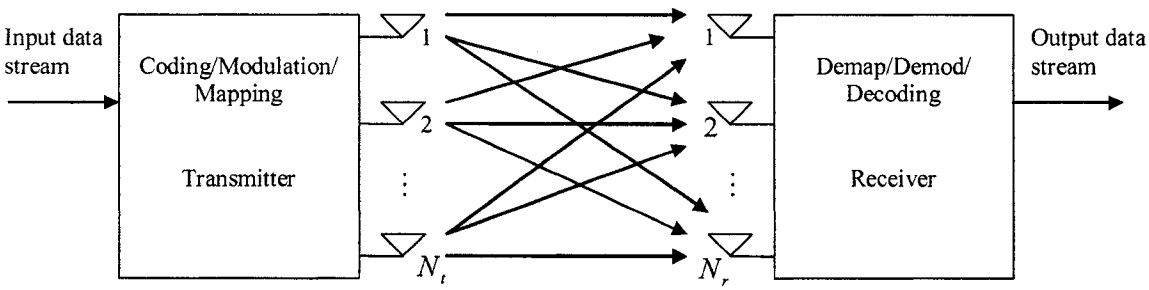

Figure 1.1: MIMO system.

1.2 Diversity Techniques

There is a high probability that a path will experience deep fade in the wireless channel. When the path is in deep fade, the signal transmitted will arrive at the receiver with error. A

solution to this problem would be to transmit the signal through multiple independent fading paths carrying the same information, and thus the probability of encountering a deep fade will be minimized. This technique is called diversity. Thus, diversity techniques will ensure that the reliability of transmission is held by combating fading and interference, without increasing the transmitted power or sacrificing the bandwidth.

There exist several types of diversity techniques, the three major types are time diversity, space diversity and frequency diversity.

1.2.1 Time Diversity

By transmitting duplicate messages in diverse time slots, time diversity is realized. This phenomenon results in uncorrelated fading signals at the receiver. Error control coding is frequently used in digital communication systems to supply a coding gain relative to uncoded systems. Error control coding combined with interleaving is applied in wireless communication to achieve time diversity. To ensure that the coded symbols are transmitted through independent fading gains, interleaving is applied to the codewords. Time diversity is generally successful for fast fading channels where the coherence time of the channel is small. An example is shown in Figure 1.2. In the example, the first system does not apply interleaving while the second system does. In the first system, the third codeword experiences a deep fade and will be lost in totality. In the second system where interleaving is applied, all the codewords will be conserved.

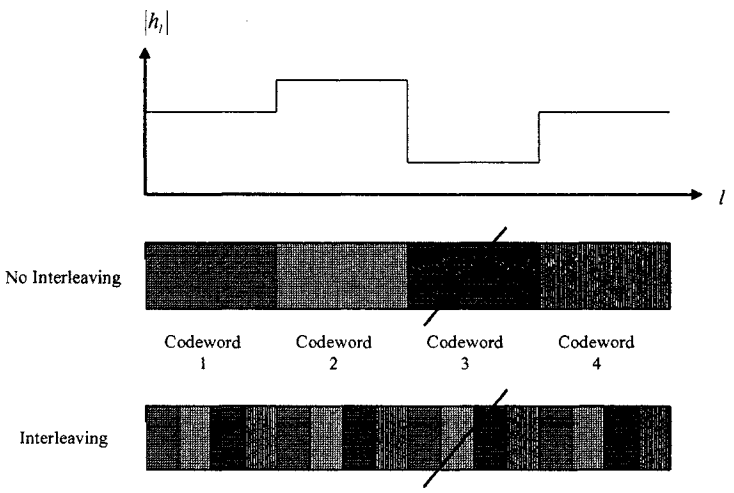

Figure 1.2: Example of the effect of interleaving codewords before transmission.

1.2.2 Space Diversity

Space diversity is obtained using multiple antennas arranged in space for transmission and/or reception. A proper distance separates the multiple antennas sufficiently far apart so that the individual signals are uncorrelated and thus the fading experienced by the different antennas will be independent. In space diversity, the duplicates of the transmitted signals are typically offered to the receiver in the method of redundancy in the space domain. Space diversity is ideal in cases where the fading is slow and interleaving over several coherence time periods is not possible. Contrasting to time and frequency diversity, space diversity does not produce any deficit in bandwidth efficiency. If multiple antennas are used at the receiver, this layout is known as receive diversity, also known as single-input multiple-output (SIMO) channels. If multiple antennas are placed at the transmitters end, this is referred to as transmit diversity or multiple-input single-output (MISO) channel. Coding problems that exist in transmit diversity have led to space-time code (STC) design, which will be discussed in detail in Chapter 2. Channels with multiple transmit and multiple receive antennas (MIMO) offer even greater potential.

1.2.3 Frequency Diversity

Frequency diversity relies on the fact that different frequencies experience different fading. To take advantage of this fact, a number of different frequencies are used to transmit the same message. In order to ensure that the fading related with different frequencies are independent, the carrier frequencies must be separated of the order of several times the channel coherence bandwidth.

In practice, not all types of diversity may be applied due to the features of the channel available and the signaling used. For example if the channel is slow fading and thus has a long coherence time, it will not support time diversity, which requires interleaving. Correspondingly, frequency diversity is impossible when the coherence bandwidth of the channel is close or equal to the signal bandwidth. Nonetheless, regardless of the channel properties, space diversity can always be effectively realized by ensuring that the multiple antennas are placed suitably distant of each other. Moreover, space diversity does not present any shortfall of bandwidth efficiency as time or frequency diversity do.

1.3 Space-time Coding

Space-time coding (STC) is a coding technique intended for use with multiple transmit and receive antennas. Applying STC to MIMO systems maximizes the capacity of the MIMO wireless channel. Coding is accomplished in both spatial and temporal domains. This is done to establish correlation among signals coming from different antennas and signals coming at different times. There exists several variations to space-time codes, these includes space-time trellis codes (STTC), space-time block codes (STBC) and layered space-time (LST) codes.

STC codes may be divided into two categories, those that provide transmit diversity gain and those that provide spatial multiplexing gain. The two main types of STC that achieve transmit diversity are STTC and STBC, while STC design that provides spatial multiplexing gain is the LST. Hence while the STTC and STBC schemes can provide full transmit diversity the highest rate offered by these schemes is unity. This is contrary to the LST scheme where no transmit diversity is achievable but full spatial multiplexing gain is.

1.4 Spatial Multiplexing

Another advantage of MIMO channels is its ability to provide a supplementary feature for communication systems, which produces a degree of freedom gain. These supplementary degrees of freedom can be taken advantage of to provide spatial multiplexing. The basic concept of spatial multiplexing is to divide a data stream into several branches and transmit them simultaneously through independent channels. Specifically, the data stream is divided into N_t data streams in a MIMO system with N_t transmit antennas. Consequently, the throughput becomes N_t symbols per channel use. This happens to be N_t times more than the rate of the STBC.

The Bell-labs layered space-time (BLAST) architecture proposed by Foschini in [4], was the first architecture to exploit the concept of spatial multiplexing and render high data rate transmission possible. Although the BLAST architecture provides high data rate transmission, it lacks in diversity gain. Specifically the BLAST scheme does not provide any transmit diversity but does provide receive diversity on some streams depending on the receiver structure.

1.5 Rate Diversity Trade-off

As discussed in previous sections, a MIMO system can provide two types of gains: diversity gain and spatial multiplexing gain. In a MIMO system with N_t transmit and N_r receive antennas, the maximum diversity gain achieved is $N_t N_r$, which is the total number of fading gains that one can average over in the channel. Earlier and some current research works in wireless communications deal with designing schemes to obtain either maximal diversity gain or obtain maximal spatial multiplexing gain. It has been shown that in a MIMO system, both gains may be exploited but there is an elementary trade-off between the spatial multiplexing gain and diversity gain [9]. Thus, increasing one type of gain will affect the other. Consequently, if a system needs to capture higher spatial multiplexing gain, this will surely decrease the diversity gain that the system can attain. The trade-off between the spatial multiplexing gain and diversity gain can be translated to the trade-off between the rate and error probability (reliability) of a MIMO system. In today's applications, it is important to acquire high data rates while maintaining good reliability of the signal. An understanding of the optimal trade-off between the rate and diversity gain of a MIMO system is crucial in order to make comparison between different architectures to ensure the adequate choice of a scheme to match the application that is required.

1.6 Aims and Outline of Thesis

This section presents the motivation behind the research work in this thesis. We wish to find MIMO systems, which provide the best spatial rate and spatial diversity gain trade-off while maintaining low complexity. The LST codes and STBCs described in the above sections are the best STC schemes in terms of complexity to provide high data rate transmission and diversity gain, respectively. Both schemes take advantage of low complexity linear processing at the receiver. By combining LST and STBC schemes, we can capitulate both gains simultaneously.

1.6.1 Thesis Contribution

The main contributions of this thesis are:

- Evaluation of detection algorithms for all BLAST schemes. The results demonstrate that the performances of suboptimal linear detectors are limited by the performance of the first detected layer without sorting. The best performance is mainly generated

by detectors following the MMSE criterion with interference cancellation techniques involved.

- Development of a new reduced complexity detection algorithm for multilayered STBC (MLSTBC). This algorithm is based on the MMSE criterion, and interference cancellation techniques. The algorithm is also low in computational complexity since the QR decomposition (QRD) is applied to the detector.

- Complexity study of the new detector algorithm. The study examines the effects of the number of antennas on the complexity of the detector.

- Evaluated the performance of the MLSTBC architecture in a frequency selective fading environment. The performance results demonstrate that an increase in diversity order is achieved by applying proper channel coding and interleaving techniques with the aid of orthogonal frequency division multiplexing (OFDM) technology.

- Development of a new transceiver architecture, which provides improved performance to a MLSTBC system as well as employing a reduced complexity detection algorithm to the system. Moreover, we evaluate the performance of the new transceiver architecture. The diversity order obtained for the new transceiver architecture is higher than that obtained from the original MLSTBC scheme.

- Evaluated and compared the spatial diversity-spatial multiplexing gain trade-off curves for the multilayerd STBC system and the new transceiver architecture. The trade-off curve for the new transceiver architecture is superior to that of the original MLSTBC architecture.

1.6.2 Organization of Thesis

The concepts of different STC design, which include STBC and LST architectures are presented in Chapter 2. The evaluations of the performance of the different LST (BLAST) architectures using different linear detectors are also examined in Chapter 2.

Chapter 3 presents a new reduced complexity detection algorithm for MLSTBC. This algorithm is based on the MMSE criterion and interference cancellation techniques. The algorithm is also low in computational complexity since the QRD principle is applied to the detector. A complexity study of the new detector algorithm is also included in Chapter 3.

Chapter 4 presents the MLSTBC architecture with the concatenation of OFDM technology. This is done in order to adapt the system to function in a frequency selective fading

environment. Performance analysis is included and simulation results are demonstrated.

Chapter 5 presents a new transceiver architecture, which provides improved performance to a MLSTBC system. Performance analysis of the new transceiver architecture, and the derivation and comparison of the spatial diversity-spatial multiplexing gain trade-off curves for the multilayerd STBC system and the new transceiver architecture is also presented in Chapter 5.

Finally the conclusion to the thesis is presented in Chapter 6 with future work suggestions.

Chapter 2

Space-Time Codes

STC is a coding technique intended for use with multiple transmit and receive antennas. Applying STC to MIMO systems maximizes the capacity of the MIMO wireless channel. Coding is accomplished in both spatial and temporal domains. This is done to establish correlation among signals coming from different antennas and signals coming at different times. There exists several variations to STCs, these includes STTCs, STBCs and LST codes.

STCs may be divided into two categories, those that provide transmit diversity gain and those that provide spatial multiplexing gain. The two main types of STC that achieve transmit diversity are STTCs and STBCs, while LST provides spatial multiplexing gain.

2.1 STC with Transmit Diversity

The main types of STC that provide transmit diversity gain are the STBCs and the STTCs. In 1998, Tarokh et al. introduced STTC in [5], where a trellis code is distributed over the multiple transmit antennas and multiple time slots to provide transmit diversity and coding gain. The decoding complexity of STTC increases exponentially as a function of the transmission rate and number of transmit antennas. Later, Alamouti in [6] introduced a very simple and efficient scheme known as the STBC scheme. The STBC scheme tackles the complexity problem encountered with STTC and presents a promising solution. The STBC scheme employs a block code in the form of a transmission matrix to solely provide to the system transmit diversity but at a much lower decoding complexity cost than in the STTC case. The Alamouti scheme is one of the simplest STC structures and is designed for two transmit antennas that could be further generalized to more than two transmit antennas, which Tarokh et al. accomplished in [7].

2.1.1 Alamouti Scheme

In the Alamouti scheme, the encoder maps data into a code matrix as

$$\mathbf{X} = \begin{bmatrix} x_1 & -x_2^* \\ x_2 & x_1^* \end{bmatrix}.$$

The rows in the coded transmission matrix $\mathbf{X}$ represent the data transmitted from the first and second antenna, respectively and the columns of the matrix represent data transmitted at time t_1 and t_2, respectively [8]. This realization of the matrix allows for the time and space diversity of the STBC to be implemented. The transmission matrix $\mathbf{X}$ is orthogonal. This design property allows for the achievement of maximum likelihood decoding with linear processing per transmitted symbol. This establishes the simplicity of the decoding process. A block diagram of the STBC transmitter structure is shown in Figure 2.1.

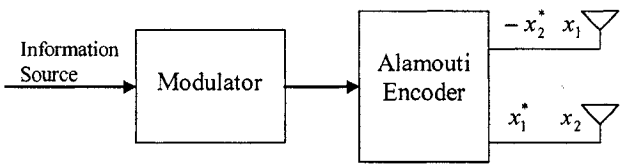

Figure 2.1: The Alamouti scheme.

The coded matrix $\mathbf{X}$ passes through a quasi-static flat fading channel, each antenna goes through a different path to reach the receiver. The channel fading coefficient matrix may be represented as

$$\mathbf{H} = \begin{bmatrix} h_{1,1} & h_{1,2} \\ \vdots & \vdots \\ h_{N_r,1} & h_{N_r,2} \end{bmatrix},$$

where $\mathbf{H}$ is the fading coefficient matrix of size $N_r \times N_t$. The matrix $\mathbf{H}$ is composed of elements $h_{j,i}$ representing the fading gains from the ith transmit antenna to the jth receive antenna. These fading coefficients are assumed to be independent and $\mathcal{CN}(0,1)$ distributed. At the receiver, the received signal may be represented as

$$\mathbf{Y} = \mathbf{HX} + \mathbf{N}$$

$$\mathbf{Y} = \begin{bmatrix} y_1(1) & y_1(2) \\ \vdots & \vdots \\ y_{N_r}(1) & y_{N_r}(2) \end{bmatrix} = \begin{bmatrix} h_{1,1} & h_{1,2} \\ \vdots & \vdots \\ h_{N_r,1} & h_{N_r,2} \end{bmatrix} \begin{bmatrix} x_1 & -x_2^* \\ x_2 & x_1^* \end{bmatrix} + \begin{bmatrix} n_{1,1} & n_{1,2} \\ \vdots & \vdots \\ n_{N_r,1} & n_{N_r,2} \end{bmatrix},$$

where $y_j(t)$ is the received signal term at receive antenna j at time t. $\mathbf{N}$ is the additive white Gaussian noise matrix. The matrix $\mathbf{N}$ is composed of elements $n_{j,i}$ representing the additive white Gaussian noise term from the ith transmit antenna to the jth receive antenna. The matrix $\mathbf{N}$ is composed of $\mathcal{CN}(0, N_0)$ distributed noise samples.

2.1.2 Alamouti Detection

The decoder uses a maximum likelihood decoder assuming that all the signals in the modulation constellation have the same probability to occur [8]. The detector constructs two decision statistics on the transmitted symbols, based on the linear combination of the received signals. The decision statistics are thus found by using the orthogonal properties of the transmitted matrix $\mathbf{X}$ as

$$\tilde{\mathbf{X}} = \begin{bmatrix} \tilde{x}_1 \\ \tilde{x}_2 \end{bmatrix} = \mathbf{H}^H \mathbf{Y}.$$

For example for a system using the Alamouti scheme (two transmit) with one receive antenna, the signal at the receiver at time T and $T + t$ may be represented as

$$\mathbf{Y} = \begin{bmatrix} y_1 \\ y_2 \end{bmatrix} = \begin{bmatrix} h_{1,1}x_1 + h_{1,2}x_2 + n_1 \\ -h_{1,1}x_2^* + h_{1,2}x_1^* + n_2 \end{bmatrix}.$$

The decoder than proceeds to make decision statistics of the received signal, the decision statistics would be

$$\tilde{\mathbf{X}} = \begin{bmatrix} \tilde{x}_1 \\ \tilde{x}_2 \end{bmatrix} = \begin{bmatrix} h_{1,1}^* y_1 + h_{1,2} y_2^* \\ h_{1,2}^* y_1 - h_{1,1} y_2^* \end{bmatrix}.$$

The estimated symbols then pass to the maximum likelihood decoder where hard decisions are made.

The Alamouti scheme can accommodate multiple receive antennas. For example in the case of two receive antennas the receiver now receives four different messages. These messages account for the different time and different antennas that they reach. If $y_{1,j}$ and $y_{2,j}$ are represented as the received signals, j signifies the antenna that received these signals at time T and $T + t$. Hence for a two receive system, there will be received messages $y_{1,1}$, $y_{2,1}$, $y_{1,2}$,

and $y_{2,2}$. Thus the received signal is

$$\mathbf{Y} = \begin{bmatrix} y_{1,1} & y_{1,2} \\ y_{2,1} & y_{2,2} \end{bmatrix} = \begin{bmatrix} h_{1,1} & h_{1,2} \\ h_{2,1} & h_{2,2} \end{bmatrix} \begin{bmatrix} x_1 & -x_2^* \\ x_2 & x_1^* \end{bmatrix} + \begin{bmatrix} n_{1,1} & n_{1,2} \\ n_{2,1} & n_{2,2} \end{bmatrix}.$$

The decoder than proceeds to make decision statistics of the received signal, the decision statistics would be

$$\tilde{\mathbf{X}} = \begin{bmatrix} \tilde{x}_1 \\ \tilde{x}_2 \end{bmatrix} = \begin{bmatrix} h_{1,1}^* & h_{1,2} & h_{2,1}^* & h_{2,2} \\ h_{1,2}^* & -h_{1,1} & h_{2,2}^* & -h_{2,1} \end{bmatrix} \begin{bmatrix} y_{1,1} \\ y_{1,2}^* \\ y_{2,1} \\ y_{2,2}^* \end{bmatrix}.$$

These estimated symbols then proceed to go through the maximum likelihood detector as in the one receiver case. Figure 2.2 demonstrates the block diagram of the Alamouti decoder.

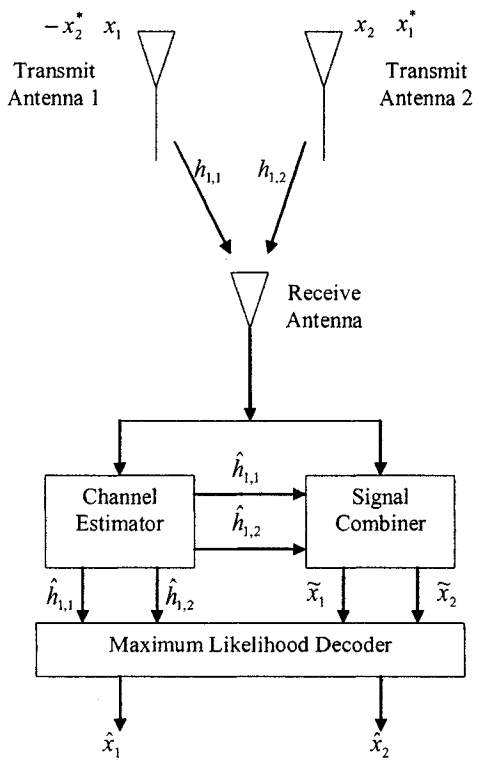

Figure 2.2: Block diagram of the Alamouti decoder

2.1.3 Generalization of STBC

The Alamouti scheme can be fashioned into a more generalized manner. This generalization will make it possible to apply STBC to more than two transmit antennas. This generalization to an arbitrary number of transmit antennas was made possible by utilizing the theory of orthogonal design. These schemes provide full diversity attainable by the number of transmit and receive antennas in the system. The generalized STBC also takes advantage of the linear processing at the receiver and uses a simple maximum likelihood decoder. It was also established in [10], that an MMSE detector may be used to successfully detect the signal.

An example of this generalization is STBC for three transmit antennas. The coded transmission matrix is [11]

$$\mathbf{X}_3 = \begin{bmatrix} x_1 & -x_2^* & x_3^* & 0 \\ x_2 & x_1^* & 0 & -x_3^* \\ x_3 & 0 & -x_1^* & x_2^* \end{bmatrix}.$$

The rows of the transmission matrix $\mathbf{X}_3$ represents the symbols transmitted by each transmit antenna. The columns represent the different time slots. Thus the required number of time slots for proper transmission is four.

2.1.4 Rate Achieved by STBC

In the STBC encoder structure, the number of symbols the encoder takes as input is K. The number of transmission periods required to transmit the STBC coded symbols is T. The rate of a STBC is the relation linking the number of input symbols to the number of new STBC symbols transmitted from all the antennas. Thus the rate is given by $R = K/T$.

For example in the Alamouti case, there are two symbols that are the input to the STBC encoder and there are two transmission periods used to transmit the STBC transmission matrix, thus the Alamouti algorithm has full rate of one. Hence the full rate is accomplished with two transmit antennas. This is the maximum rate obtained from any STBC. For higher number of transmit antennas, in order for the STBC scheme to achieve full rate the number of transmission periods must equal the number of transmit antennas. This is possible for $2, 4$ and 8 transmit antennas. Other amounts of transmit antennas do not benefit from full rate.

Consequently there is a need to find a scheme where a higher rate is available for high data rate applications. This is made possible through spatial multiplexing and is discussed in the next section.

2.2 Simulation Results for STBC

In this section we present simulation results for the STBC scheme. For all the simulation results we employed the BPSK modulation, and we assume perfect channel knowledge at the receiver and that the channel is quasi-static. We demonstrate the bit error rate (BER) vs. the signal to noise ratio (SNR) results, where $\rho = \frac{E_b}{N_0}$.

In Figure 2.3 we plot the simulation results for the STBC scheme for $N_t = 2, 3, 4$ transmit antennas, respectively, and one receive antenna. The simulation results demonstrate that by adding a transmit antenna we increase the diversity order linearly. Hence the diversity order for a 2×1 STBC MISO system is 2, 3×1 STBC MISO system diversity is 3, and for a 4×1 STBC MISO system the diversity order is 4.

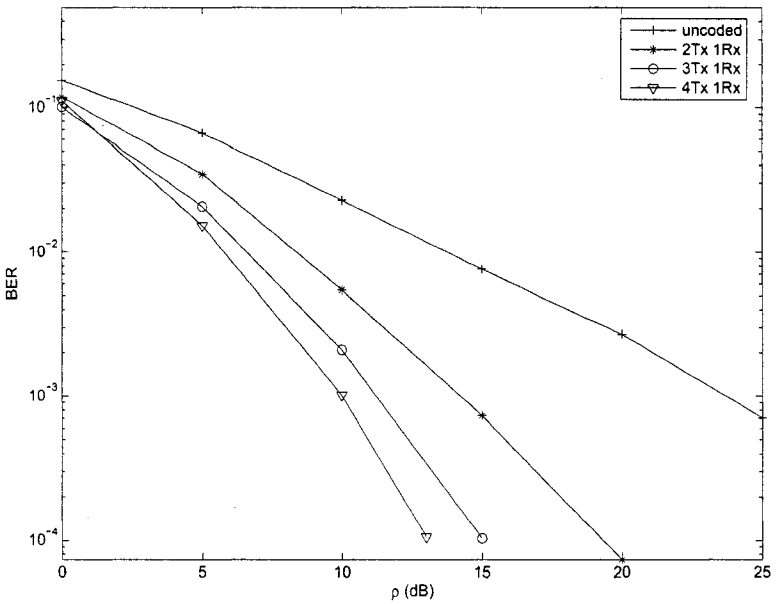

Figure 2.3: BER performance results of the STBC scheme with variable number of transmit antennas and one receive antenna.

In Figure 2.4 we demonstrate the simulation results of the STBC scheme with $N_t = 2$, and $N_r = 1$ and 2 receive antennas respectively. From the simulation results presented in the figure, it is obvious that by adding a receive antenna the diversity order increases. Hence the diversity order of the 2×1 system is 2 while that of the 2×2 MIMO system experiences a diversity order of 4.

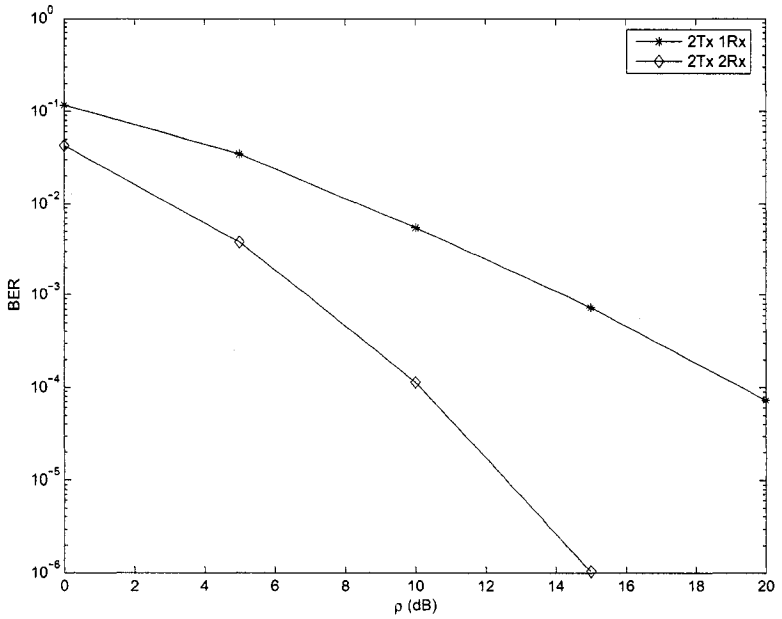

Figure 2.4: BER performance results for STBC scheme with one and two receive antennas.

2.3 Layered Space-time Coding

The STBC scheme provides full transmit diversity gain but lacks the ability to provide high data rate transmission to a wireless communication system. This is because STBC lacks in multiplexing gain. The LST code proposed by Foschini in 1998 (also called the BLAST architecture) [4] was designed to offer a MIMO system with spatial multiplexing gain. This is accomplished by demultiplexing the incoming data stream into N_t sub-streams before transmission. Symbols are transmitted simultaneously through all transmit antennas. The receiver applies successive interference cancellation (SIC) detection techniques to detect symbols and eliminate interference from other transmitted layers by applying $N_r \geq N_t$ receive antennas. The detector uses linear techniques such as the zero-forcing (ZF) and minimum mean square error (MMSE) detectors, which decrease the complexity of the system in comparison to the maximum likelihood (ML) detector [12].

In this section, an overview of LST architectures is presented. There exists different types of BLAST architectures, including the Diagonal BLAST (D-BLAST), Vertical BLAST (V-BLAST), and finally Horizontal BLAST (H-BLAST). Different detection techniques are also studied which are used in the detection process of LST schemes. Further, simulation results of the different LST architectures and different detection algorithms are evaluated.

2.3.1 V-BLAST

In the V-BLAST scheme, each transmit antenna is devoted to one layer, thus the layers are vertically positioned. In the V-BLAST architecture, the incoming data stream is demultiplexed into N_t substreams referred to as layers. Each layer is organized in frames of length L The N_t layers, are modulated separately and transmitted simultaneously by independent transmit antennas. A block diagram of the V-BLAST is shown in Figure 2.5.

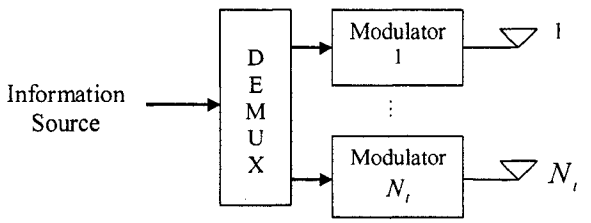

Figure 2.5: V-BLAST transmitter structure.

The modulated symbols are arranged in a transmission matrix of size $N_t \times L$ as

$$\mathbf{X} = \begin{bmatrix} x_{1,1} & \cdots & x_{1,L} \\ \vdots & \ddots & \vdots \\ x_{N_t,1} & \cdots & x_{N_t,L} \end{bmatrix}.$$

Each row represents the symbols transmitted by each transmit antenna. That is, a transmission matrix entry $x_{i,t}$ is transmitted from antenna i at time t.

2.3.2 H-BLAST

When channel coding is introduced to the V-BLAST system, the scheme becomes known as the H-BLAST architecture. Each layer is encoded separately by a channel encoder, interleaved, modulated and then transmitted as shown in Figure 2.6. It is usually assumed that the channel encoders of every layer are identical, but this may be changed.

Several differences exist between the V-BLAST and D-BLAST schemes. The transmitted layers of the V-BLAST scheme can be coded or uncoded, while the D-BLAST scheme is intended to be used only with coded layers. Consequently, this is the purpose behind cycling, which offers added spatial diversity for each layer especially over slowly fading channels [13]. Additionally, each layer in the D-BLAST scheme profits from equal diversity order due

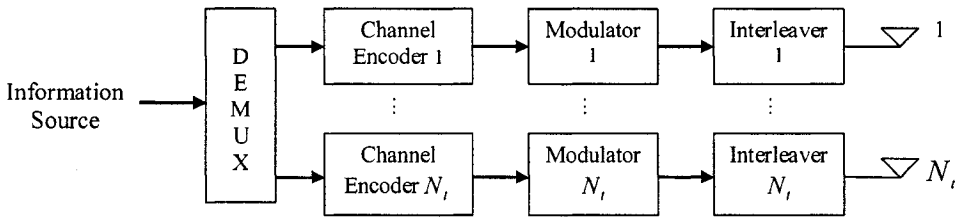

Figure 2.6: H-BLAST transmitter structure

to the diagonal structure of its transmission matrix, whereas the V-BLAST layers have unequal diversity orders. Nonetheless, D-BLAST requires advanced coding techniques at the transmitter to optimize the performance of the code across space and time [14], which adds complexity to the system. Also, D-BLAST experiences some rate deficiency since in the diagonalization stage some of the antennas transmit nothing.

2.3.3 D-BLAST

The D-BLAST architecture was originally proposed by Foschini in 1996 [4]. The vertical version of the BLAST was proposed by [2] as a simplification of D-BLAST.

In the D-BLAST architecture, the incoming data stream is demultiplexed into N_t sub-streams referred to as layers. The layers are then dispersed between the N_t transmit antennas in a diagonal fashion across space and time. The different transmitting antennas transmit each diagonal, so the first diagonal is transmitted through the first antenna, the second diagonal by the second antenna and so on.

For example in a system with four transmit antennas the V-BLAST transmission matrix $\mathbf{X}$ is

$$\mathbf{X} = \begin{bmatrix} x_{1,1} & x_{1,2} & x_{1,3} & \cdots \\ x_{2,1} & x_{2,2} & x_{2,3} & \cdots \\ x_{3,1} & x_{3,2} & x_{3,3} & \cdots \\ x_{4,1} & x_{4,2} & x_{4,3} & \cdots \end{bmatrix},$$

whereas the D-BLAST transmission matrix will be

$$\mathbf{X} = \begin{bmatrix} x_{1,1} & x_{1,2} & x_{1,3} & \cdots & \cdots & \cdots \\ 0 & x_{2,1} & x_{2,2} & x_{2,3} & \cdots & \cdots \\ 0 & 0 & x_{3,1} & x_{3,2} & x_{3,3} & \cdots \\ 0 & 0 & 0 & x_{4,1} & x_{4,2} & x_{4,3} \end{bmatrix}.$$

This scheme creates space diversity, which is not present in the V-BLAST and H-BLAST schemes and gives better performance.

2.4 Receiver Structures

2.4.1 Zero-Forcing BLAST Detection

Assuming quasi-static flat fading channel, the received signal of a BLAST scheme may be expressed as

$$\mathbf{Y} = \mathbf{HX} + \mathbf{N},$$

where $\mathbf{H}$ is the fading coefficient matrix of size $N_r \times N_t$, and $\mathbf{N}$ is the additive white Gaussian noise matrix. The matrix $\mathbf{H}$ is composed of elements $h_{i,j}$ representing the fading gains from the jth transmit antenna to the ith receive antenna. These fading coefficients are assumed to be independent and $\mathcal{CN}(0,1)$ distributed. The matrix $\mathbf{N}$ is composed of $\mathcal{CN}(0,N_0)$ distributed noise samples with a size of $N_r \times L$.

In [12] Foschini et al. proposed the BLAST receiver that is founded on a mixture of interference suppression and cancellation techniques. Each transmitted layer is taken into account one at a time to be the sought out symbol while the rest is considered as interferers. The interferers are nulled (suppressed) by a zero-forcing (ZF) matrix. The ZF criterion establishes that the mutual interference between all layers shall be perfectly suppressed. The Moore-Penrose pseudo-inverse of the channel matrix that is denoted by $\mathbf{H}^{\dagger}$ accomplishes this. The ZF filter matrix may be expressed as

$$\mathbf{G}_{ZF} = \mathbf{H}^{\dagger} = (\mathbf{H}^H\mathbf{H})^{-1}\mathbf{H}^H. \tag{2.1}$$

From the ZF filter matrix, we observe that small eigenvalues of $\mathbf{H}^H\mathbf{H}$ will lead to large errors due to noise amplification. In order to improve the performance, the noise term can be included in the design of the filter matrix $\mathbf{G}$. This is accomplished by the MMSE detection criterion, where the MMSE filter represents an exchange between noise amplification and interference suppression. The MMSE detector will be examined in another section. Also, a much lower complexity method to compute the ZF criterion is accomplished with the QR decomposition as examined in the next section.

The first step in the detection process is to create decision statistics, which are found by

passing the received signal matrix $\mathbf{Y}$ through the ZF filter matrix $\mathbf{G}_{ZF}$ as

$$\tilde{\mathbf{X}} = \mathbf{G}_{ZF}\mathbf{Y} = \mathbf{X} + (\mathbf{H}^H\mathbf{H})^{-1}\mathbf{H}^H\mathbf{N}. \tag{2.2}$$

The received matrix $\mathbf{Y}$ contains residual interference coming from the other transmitted layers. A decision will be made from the acquired statistics for the desired layer; its interference contribution is then calculated and subtracted from the received matrix $\mathbf{Y}$ as

$$y_{i,t} = y_{i,t} - \sum_{k=i+1}^{N_t} h_{i,k}\hat{x}_{k,t},$$

where the term $y_{i,t}$ is the element from the $\mathbf{Y}$ matrix found at the tth column and ith row, and $\hat{x}_{k,t}$ is the hard decision of the transmit signal $x_{k,t}$. The received matrix will now have a reduced amount of interference and hence will increase the probability of a correct detection to occur in the successive layers. Following this step, the ith column of the channel matrix $\mathbf{H}$ is set to zero. Thereafter, the pseudo inverse of the reduced channel matrix $\mathbf{H}$ is utilized to obtain the nulling vector for the next detection stage. The first detected layer is N_t until layer 1 is detected for an unordered system. In order to achieve the best performance, it is optimal to choose the layer with the largest post detection SNR or equivalently with the smallest estimation error. Consequently it is optimal to choose the row of $\mathbf{G}_{ZF}$ with minimal norm and then detect the related layer in detection step i. The sequence $K = (k_1, k_2, k_3, \ldots, k_{N_t})$ is the detection order of N_t layers, and k_i is the symbol index detected at the ith stage.

The major disadvantage of the BLAST detection algorithm is its computational complexity, since it needs multiple computation of the pseudo-inverse of the channel matrix [15].

The ZF detector works only on systems where the number of receive antennas is equal or larger than the number of transmit antennas. An additional disadvantage to this scheme is that attainable diversity depends on distinct layers. The diversity order of the ith layer, d_i can be expressed as follows [16], [17], [18]

$$d_i = N_r - i + 1, \tag{2.3}$$

where N_r is the number of receive antennas and i is the layer being detected. For example, at layer N_t, the first detected layer, $(N_t - 1)$ layers need to be suppressed, and so the diversity will be $d_4 = 1$ (assuming $N_r = N_t$). In the first layer, there are no interferers to be suppressed and thus the diversity is $d_1 = N_r = N_t$. Diagonal layering is thus needed to achieve equal

performance across the layers [9].

2.4.2 Zero-Forcing BLAST with QR Decomposition

In order to significantly reduce the computational effort of detection, we can use the QR decomposition (QRD). By decomposing the channel matrix $\mathbf{H}$ into $\mathbf{H} = \mathbf{QR}$ where $\mathbf{Q}$ is an $N_r \times N_t$ unitarian matrix and $\mathbf{R}$ is an $N_t \times N_t$ upper triangular matrix. Multiplying the received signal $\mathbf{Y}$ with the Hermitian of $\mathbf{Q}$ we obtain

$$\mathbf{Y}' = \mathbf{Q}^H\mathbf{Y} = \mathbf{RX} + \mathbf{Q}^H\mathbf{N} = \mathbf{RX} + \boldsymbol{\eta}.$$

Since $\mathbf{Q}$ is unitary, the statistical properties of the noise term $\boldsymbol{\eta}$ remain unaffected. If we expand $\mathbf{Y}'$ we can better examine what is happening to the received matrix.

$$y'_{i,t} = r_{i,i}x_{i,t} + \sum_{k=i+1}^{N_t} r_{i,k}x_{k,t} + \eta_{i,t}.$$

The first part of the equation represents the desired symbol followed by the second part which is the interference. The term $r_{i,i}$ is the element from the $\mathbf{R}$ matrix found at the ith column and ith row [15]. From this expansion we see that to obtain the desired symbol we must cancel the interference part and thus the estimated symbol vector will be

$$\tilde{x}_{i,t} = r_{i,i}x_{i,t} + \sum_{k=i+1}^{N_t} r_{i,k}(x_{k,t} - \hat{x}_{k,t}) + \eta_{i,t},$$

which may be re-written as

$$\tilde{x}_{i,t} = y'_{i,t} - \sum_{k=i+1}^{N_t} r_{i,k}\hat{x}_{k,t}.$$

The first layer detected is N_t due to the upper triangular properties of the matrix $\mathbf{R}$. The $(N_t - 1)$th layer is subsequently detected. This process continues until the first layer is detected.

2.4.3 MMSE Detector

The MMSE detector minimizes the mean squared error linking the transmitted symbols and the output of the linear detector. The MMSE filter matrix is expressed as

$$\mathbf{G}_{MMSE} = (\mathbf{H}^H\mathbf{H} + \delta_n^2\mathbf{I}_{N_t})^{-1}\mathbf{H}^H,$$

where δ_n^2 is the noise variance and $\mathbf{I}_{N_t}$ is a $N_t \times N_t$ identity matrix.

As in the ZF detector case, the decision statistics are obtained by multiplying the received matrix $\mathbf{Y}$ by the MMSE filter matrix as

$$\tilde{\mathbf{X}} = \mathbf{G}_{MMSE}\mathbf{Y}.$$

The hard decisions are then obtained from the decision statistics and in turn its interference contribution is calculated and subtracted from the received signal, as in the previous section. The MMSE filter matrix must be re-computed with the newly calculated received matrix and the process is continued until all layers are decoded [15].

2.4.4 Sorted QR Decomposition

The order of the detection process is a crucial factor in the error probability performance. In order to enhance the error probability obtained from the BLAST schemes, it is optimal to choose and detect the layer with the largest post detection SNR first. Thus, we place the weaker layers later in the detection process, since the overall system performance is limited by the performance of the first detected layer.

It is quite simple to achieve this strategy. We must first order the channel matrix $\mathbf{H}$ with columns having smallest norms first to highest values of column norms. Thus, we can find the order of detection k for $i = 1, \ldots, N_t$ to be

$$k_i = \arg \min_{l=i, \ldots, N_t} \|h_l\|^2,$$

where h_l represents the lth column of the channel matrix $\mathbf{H}$, and $\|\cdot\|$ represents the norm operation. Once the sorted channel matrix $\mathbf{H}$ is found, we apply the QRD to the channel matrix $\mathbf{H}$ to obtain new $\mathbf{Q}$ and $\mathbf{R}$ matrices. The new $\mathbf{R}$ matrix will have a property that r_{N_t,N_t} will be maximized over the entire potential combination of the columns of the channel matrix $\mathbf{H}$, followed by r_{N_t-1,N_t-1}, until we reach $r_{1,1}$, which will have the lowest value. This algorithm optimizes the detection sequence by using a single sorted QRD and thus reduce the computational complexity compared to the ZF-BLAST algorithm.

2.5 Simulation Results for BLAST schemes

In this section the simulation results for the various BLAST schemes along with the different detection algorithms are demonstrated. The BLAST schemes were simulated with $N_t = 4$

transmit antennas and $N_r = 4$ receive antennas, using BPSK modulation, with frame length $L = 100$.

In Figure 2.7, we plot the BER of the different detection algorithms that include the zero forcing (ZF) algorithm (using the Pseudo-Inverse of the channel matrix) the ZF with interference cancellation (ZF-IC), the, MMSE and the MMSE-IC detectors for an uncoded V-BLAST system. Also included in Figure 2.7 is the interference free bound (IFB) BER performance, which is given by

$$P_b \approx \binom{2N_r - 1}{N_r} (4\rho)^{-N_r},$$

where $\rho = \frac{E_b}{N_0}$. The IFB reference is for four receive antennas and one transmit antenna, since no transmit diversity is obtained from V-BLAST. From Figure 2.7, the results confirm that with IC added to the detectors, an increase in performance is accomplished. From the figure, it is also evident that the MMSE detector has better performance results than that of the ZF detector.

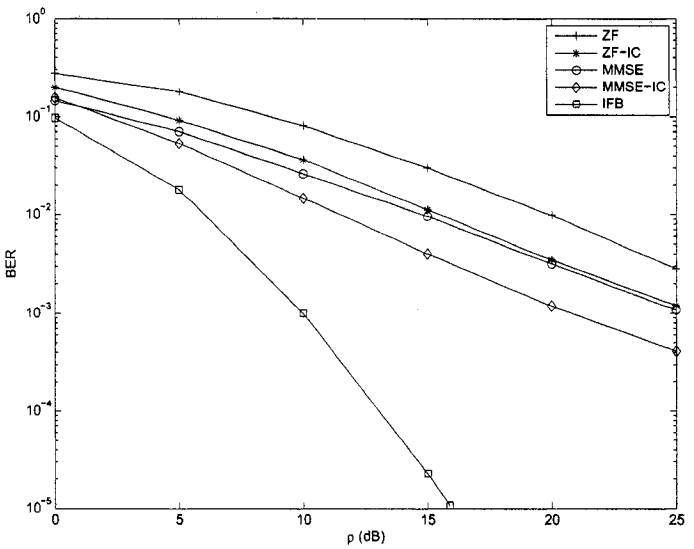

Figure 2.7: BER perfromance of V-BLAST scheme with different detectors.

In Figure 2.8 we demonstrates a V-BLAST architecture using the ZF-IC detector. The "genie" method is employed, which means that it is assumed that all detected symbols from previous layers are correct and without errors. Using this method, we can see the different diversity attained by the different layers. It is clear from Figure 2.8 that the first detected layer has the lowest diversity and this diversity increase as we move from one layer to another

as in (2.3). Thus the first detected layer in an unsorted algorithm will have $d_4 = 1$, and the last layered detected will have $d_1 = 4$.

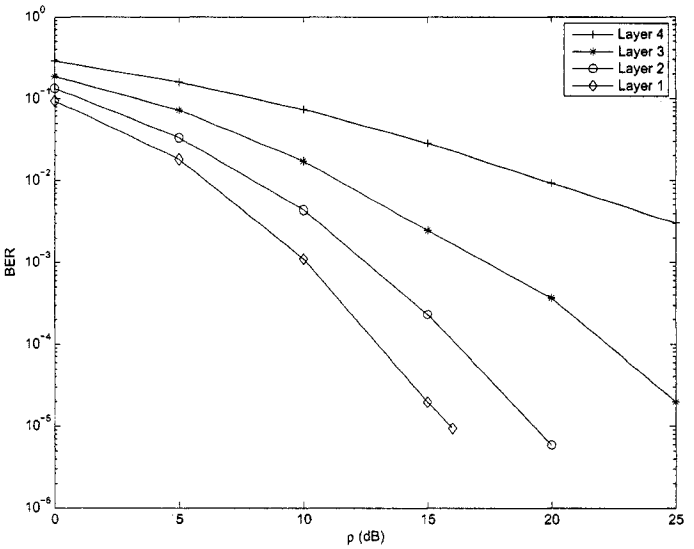

Figure 2.8: BER performance of different layers in a V-BLAST scheme.

In Figure 2.9 we demonstrate another set of different detector that apply the ZF criterion on an uncoded V-BLAST system. The detectors covered in Figure 2.9 are the ZF (Pseudo-Inverse), the ZF-IC (QRD), the sorted QRD (SQRD), and finally the original V-BLAST detector as described in section 2.4.1. From Figure 2.9, we see that the SQRD decoder results in increased performance compared to the QRD decoder without sorting. The SQRD achieves a performance gain of 1dB at BER $\sim 10^{-3}$ compared to the unsorted QRD algorithm. The SQRD method almost attains the same performance as the original V-BLAST decoder implemented by Foschini but SQRD has a much lower complexity then the original V-BLAST decoder. There is $\sim 8dB$ increase in performance between the SQRD algorithm and that of the ZF with Pseudo inverse algorithm.

In Figure 2.10 we plot the same set of detectors as in Figure 2.9, but the detector is following the MMSE criterion. Also shown in the same figure is the BER results of the last detected layers of the V-BLAST scheme. We arrive at the same conclusion from the simulation results shown in Figure 2.10 as those pulled from Figure 2.9, which is that the sorted algorithm performs better. In this case a much greater performance improvement is established. A performance gain of $\sim 7dB$ is obtained using the SQRD compared to the QRD algorithm.

In Figures 2.11 we present the simulation results of the SC-BLAST scheme with the ZF,

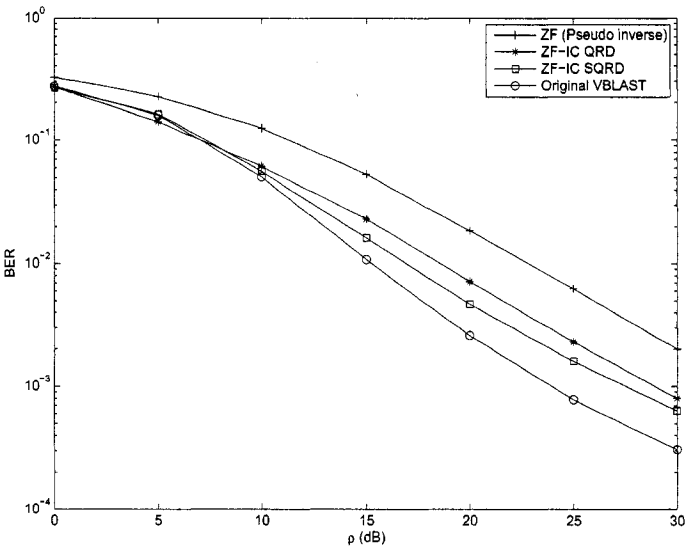

Figure 2.9: BER performance of V-BLAST with different detectors following the ZF criteria.

ZF-IC, MMSE, and MMSE-IC detectors. The figure further justify that the MMSE detectors perform better than the ZF detectors and that IC aids in better detection. Specifically in Figure 2.11, a performance gain of $\sim 7dB$ is attained using the MMSE-IC algorithm compared to the ZF-IC algorithm.

In Figure 2.12 we demonstrate the performance results of the H-BLAST scheme with the ZF, ZF-IC, MMSE, and MMSE-IC detectors. An interesting observation is found in Figure 2.12, which is that the ZF-IC and MMSE detection algorithms attain the same performance.

In Figure 2.13 we depict the simulation results of the D-BLAST scheme with the ZF, ZF-IC, MMSE, and MMSE-IC detectors. In Figure 2.13, there is an immense performance gain between the MMSE-IC and ZF-IC algorithm. The results demonstrate a $15dB$ gain between the MMSE-IC and ZF-IC detectors.

In Figure 2.14 we demonstrates the BER performance of the first and last layers detected for the D-BLAST and H-BLAST schemes employing the "genie" detection. From the Figure, it is obvious that the D-BLAST scheme has an advantage over the H-BLAST scheme, in that the all the layers detected have the same performance. In the H-BLAST scheme, the first layer and last layer do not share the same diversity order. Having the same performance through out the layers is advantageous in a multiuser system, where all users will have equal performance granted.

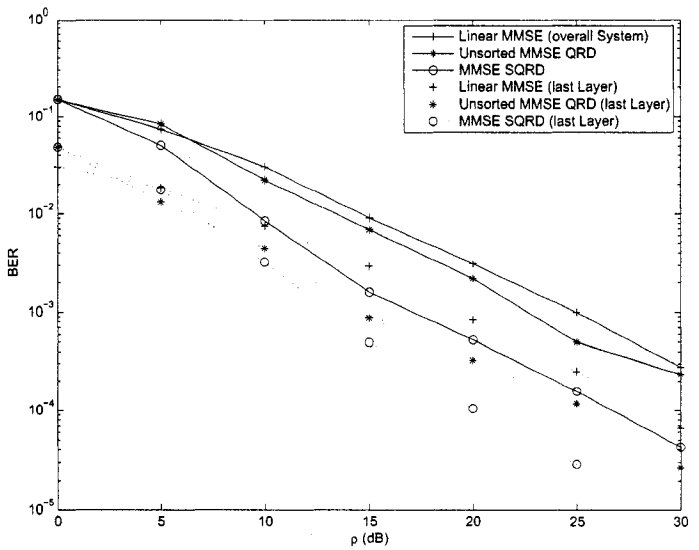

Figure 2.10: BER of V-BLAST with different detectors followoing the MMSE criterion.

In Figure 2.15 we demonstrates a comparison between the frame error rate (FER) performance results of an uncoded and coded V-BLAST system. In Figure 2.15, the ZF-SQRD detector was applied, from the Figure it is obvious that it is advantageous to add coding to the system.

In Figure 2.16 plot the simulation results of four different LST architectures all using the MMSE decoder with IC. In the simulation, error free propagation was assumed, thus the "genie" algorithm is applied. From Figure 2.16, we see that the D-BLAST architecture does in fact have the best diversity and outperforms all the other schemes. The SC-BLAST outperforms the H-BLAST and V-BLAST, because it only employs a single channel encoder that is distributed amongst all the transmitting antennas, this actually acts as diversity. However as seen in Figure 2.11, SC-BLAST is extremely responsive to interference [19].

2.6 Multilayered Space Time Coding

A multilayered space-time coding (MLSTC) architecture was introduced in [20] by Tarokh et al, to provide an improved trade-off between spatial diversity and multiplexing gain. It was also shown in [21] and [22] the MLSTC scheme with a different configuration but holding the same principles of those in [20]. The MLSTC scheme merges coding concepts at the transmitter and signal array processing at the receiver. This scheme enhances the systems performance by augmenting the spatial diversity order and increasing the spatial multiplexing

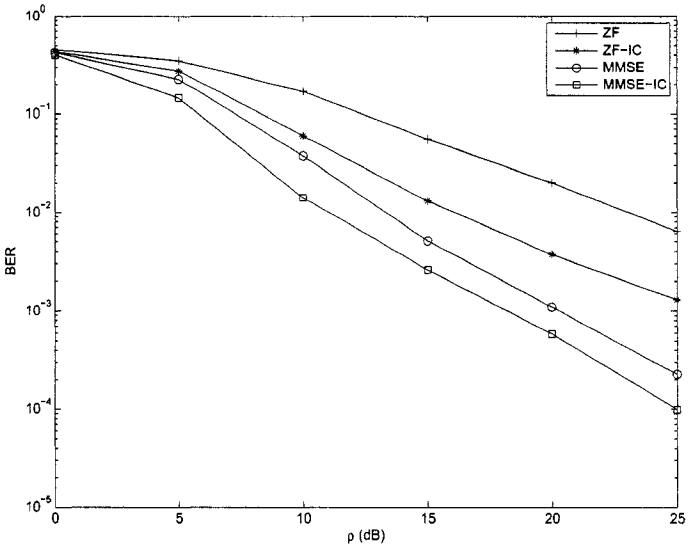

Figure 2.11: BER performance of SC-BLAST with different detectors.

gain by adopting approaches of LST coding. In particular, the MLSTC scheme divides the transmit antennas into subgroups and each subgroup has its corresponding space-time code (STC). At the receiver, each individual STC is decoded using a linear processing technique that first suppresses the signals transmitted from the other subgroups by considering them as interferers. This detection process is called the group interference cancellation (GIC) detector. With this architecture, the subgroups attain different diversity orders leading to distinct performance results from one another. The architecture of MLSTC can be viewed in Figure 2.17.

2.6.1 MLSTC System Model

The MLSTC architecture is a MIMO system with N_t transmit and N_r receive antennas. The input data stream is initially demultiplexed into N_t substreams. From this point, the layers are divided into K parallel groups. Each group is composed of a STC encoder, we will consider the case of using a STBC encoder at each layer and thus we can refer to the architecture as MLSTBC. Each group consists of n antennas, hence the total number of transmit antennas N_t is equal to Kn. The MLSTBC system can be represented as (N_t, n, N_r).

The overall transmit signal matrix can be described by stacking all the signal matrices

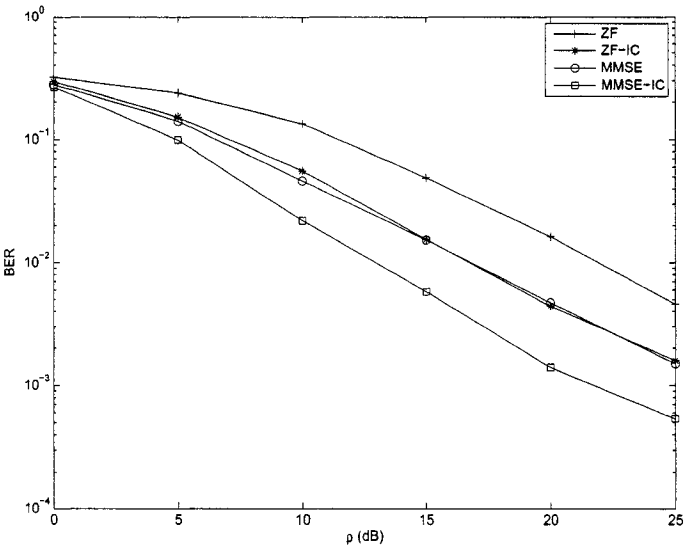

Figure 2.12: BER performance of H-BLAST with different detectors.

resulting from each STBC encoders $\mathbf{G}_i(x)$, for $(i = 1, 2, \ldots, K)$ as

$$\mathbf{G}(x) = \left[\begin{array}{cccc} \mathbf{G}_1(x) & \mathbf{G}_2(x) & \cdots & \mathbf{G}_K(x) \end{array} \right]^T.$$

For example if we were employing a $(4, 2, 4)$ system, the transmission matrix would be

$$\begin{aligned} \mathbf{G}(x) &= \left[\begin{array}{c} \mathbf{G}_1(x) \\ \mathbf{G}_2(x) \end{array} \right] \\ &= \left[\begin{array}{cc} x_1 & -x_2^* \\ x_2 & x_1^* \\ x_3 & -x_4^* \\ x_4 & x_3^* \end{array} \right], \end{aligned}$$

where the first two rows represents matrix $\mathbf{G}_1(x)$ and the next two row represent $\mathbf{G}_2(x)$.

Assuming a quasi-static flat fading channel, the received signal may now be expressed as

$$\mathbf{Y} = \mathbf{H}\mathbf{G}(x) + \mathbf{N},$$

where $\mathbf{H}$ is the fading coefficient matrix of size $N_r \times N_t$ with elements $h_{i,j}$ representing the fading gains from the jth transmit antenna to the ith receive antenna. These fading coefficients are assumed to be independent and $\mathcal{CN}(0, 1)$ distributed. The matrix $\mathbf{N}$ is

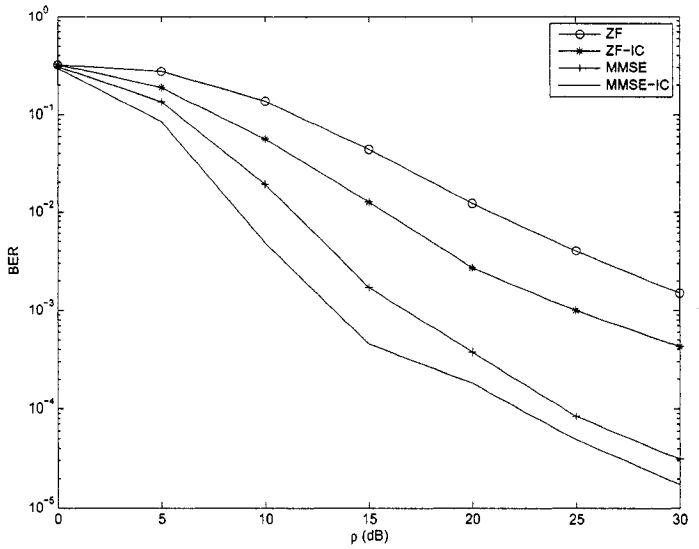

Figure 2.13: BER performance of D-BLAST with diffrent detectors.

composed of $\mathcal{CN}(0, N_0)$ distributed noise samples with a size of $N_r \times nL$.

2.6.2 MLSTC Decoder

The decoding of MLSTC is accomplished by the use of group interference suppression. This is done in order to decode each subgroup separately, and treat the other subgroups as interferers [20]. The condition for this decoding scheme to work is to ensure that $Nr \geq Nt - n + 1$.

The channel matrix can be divided into two parts, the first part will contain the channel coefficients of the subgroup that needs to be detected and the rest will be the channel coefficients of the interfering subgroups. Thus, we may write the channel matrix as

$$\mathbf{H} = [\mathbf{H}_{g_1} \mathbf{H}_{g-g_1}]$$

For example in a (4,2,4) MLSTBC scheme, we can represent the channel matrix channel by

$$\begin{aligned} \mathbf{H} &= [\mathbf{H}_{g_1} \mathbf{H}_{g_2}] \\ &= \begin{bmatrix} h_{11} & h_{12} & h_{13} & h_{14} \\ h_{21} & h_{22} & h_{23} & h_{24} \\ h_{31} & h_{32} & h_{33} & h_{34} \\ h_{41} & h_{42} & h_{43} & h_{44} \end{bmatrix}, \end{aligned}$$

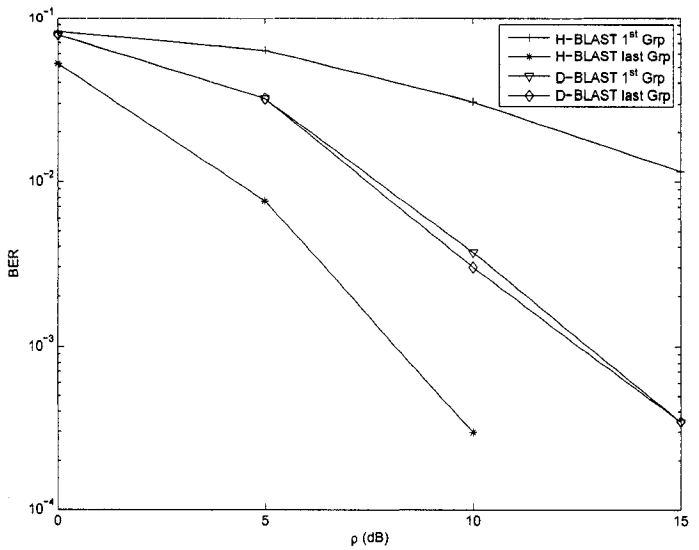

Figure 2.14: BER perfromance of the first and last layers detected for the D-BLAST and H-BLAST schemes.

where the first two columns represent $\mathbf{H}_{g_1}$ and the subsequent two columns represent $\mathbf{H}_{g_2}$.

If we wish to decode the first group and null out the second group, then a nulling matrix, which spans the null space of $\mathbf{H}_{g_2}$ is generated, such that the nulling matrix holds the following properties.

$$\mathbf{\Omega}_{g_2}\mathbf{\Omega}_{g_2}^{H} = \mathbf{I}_{N_r-N_t+n},$$

where $\mathbf{I}_{N_r-N_t+n}$ is a $N_r - N_t + n \times N_r - N_t + n$ identity matrix. Given that $\mathbf{\Omega}_{g_2}$ spans the null space of $\mathbf{H}_{g_2}$, the following must also hold

$$\mathbf{\Omega}_{g_2}\mathbf{H}_{g_2} = 0.$$

The received matrix $\mathbf{Y}$ may now be re-written as

$$\mathbf{Y} = [\mathbf{H}_{g_1}\mathbf{H}_{g-g_1}]\,\mathbf{G}(x) + \mathbf{N}.$$

If we multiply the nulling matrix $\mathbf{\Omega}_{g_2}$with the received matrix $\mathbf{Y}$, we will obtain

$$\mathbf{Y}' = \mathbf{\Omega}_{g_2}\,[\mathbf{H}_{g_1}\mathbf{H}_{g-g_1}]\,\mathbf{G}(x) + \mathbf{\Omega}_{g_2}\mathbf{N},$$

thus,

$$\mathbf{Y}'_{g_1} = \mathbf{\Omega}_{g_2}\mathbf{H}_{g_1}\mathbf{G}_1(x) + \mathbf{\Omega}_{g_2}\mathbf{N}.$$

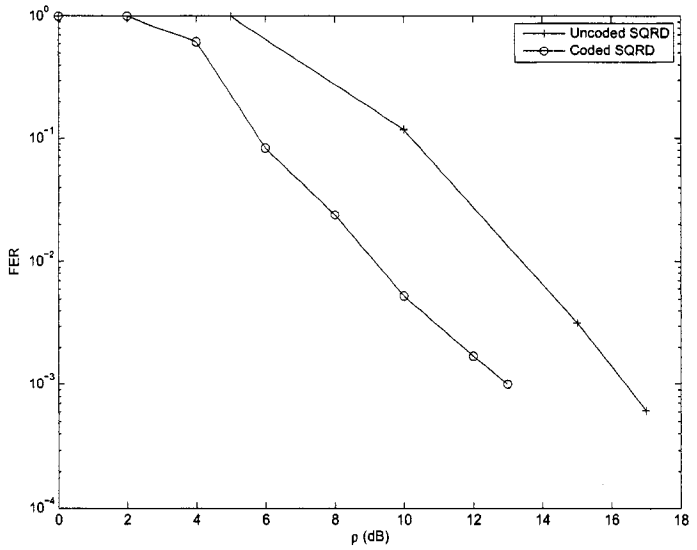

Figure 2.15: FER of coded and uncoded V-BLAST using the SQRD detector.

This nulling procedure is a main cause of receive diversity reduction [3]. Hence, the first group to be detected will take advantage of a lower diversity order than that of the second group detected.

After the first group has been detected, $\mathbf{Y}'_{g_1}$ is passed to the STBC decoder for hard decisions. Once decoded, its interference contribution is calculated and subtracted from the received signal as such

$$\mathbf{Y}' = \mathbf{Y}' - \mathbf{H}_{g_1}\hat{\mathbf{G}}_1(x).$$

We may then continue by detecting the subsequent groups as described above.

2.6.3 Diversity Achieved by the MLSTBC

The first group detected in the MLSTBC scheme achieves a diversity gain of $n_1 \times (n_1 + N_r - N_t)$, where n_k are the antennas from the kth STBC encoder. After decoding the first group and subtracting its interference from the received signal, the second group can be detected, which achieves a diversity gain of $n_2 \times (n_2 + n_1 + N_r - N_t)$. Thus, for the MLSTBC scheme using the GIC decoder, the kth detected group achieves a diversity gain of [20]

$$n_k \times (n_1 + n_2 + \cdots + n_k + N_r - N_t).$$

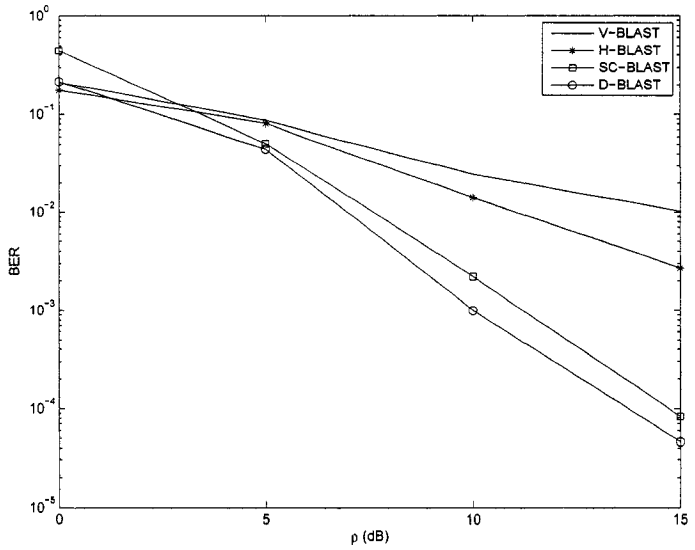

Figure 2.16: Comparison of different LST architectures.

The overall system performance is limited by the performance of the first group. Hence the overall performance of the MLSTBC architecture at high SNR values can approximated as [23]

$$P_b \approx \binom{2n(n+N_r-N_t)-1}{n(n+N_r-N_t)} (4\rho)^{-n(n+N_r-N_t)},$$

where $\rho = \frac{E_b}{N_t N_0}$.

2.7 Simulation Results of MLSTC System

In this section we present the simulation results of the MLSTBC scheme depicted in Figure 2.17. The detector applied to the simulation results is the GIC detector presented in the previous section. The channel fading coefficients remained unvarying over a block of length $L = 100$ consecutive symbols and vary independently from one block to another. BPSK modulation was applied to the system.

In Figure 2.18 we demonstrates the simulation results for a 4×4 MIMO system employing the MLSTBC architecture. In Figure 2.18, the decoder uses the "genie" method, which assumes perfect detection at previous layers, and thus perfect interference cancellation, in order to demonstrate the diversity order reached by the different layers. From the figure we see that the second group detected, takes advantage of a higher diversity order compared

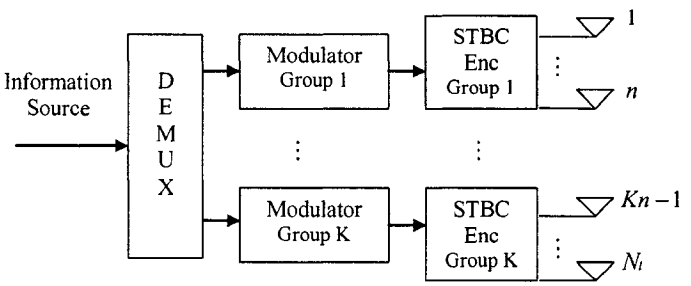

Figure 2.17: MLSTBC transmitter structure.

to the first detected group. The diversity order of the first detected group is equal to $n \times (n + N_r - N_t)$, hence for the system simulated here the first group has diversity gain equal to 4. The second group has diversity gain equal to $n \times (2n + N_r - N_t)$, thus it achieves a diversity gain of 8, which is a significant increase.

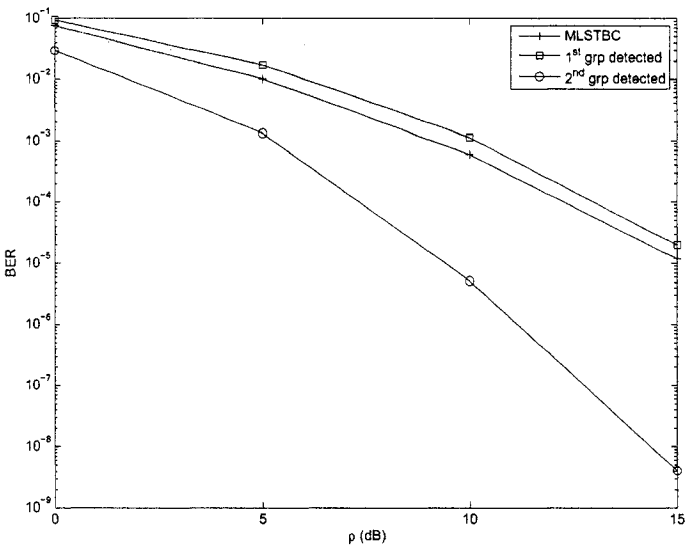

Figure 2.18: BER performance of MLSTBC with "genie" detection.

In Figure 2.19 we demonstrate the simulation results for a 4×4 MLSTBC system with error propagation at each layer. From the figure it is evident that the second layer achieves a better performance than the first layer detected. We also observe that with error propagation at each detection stage the IC detection algorithm is able to properly detect the transmitted messages.

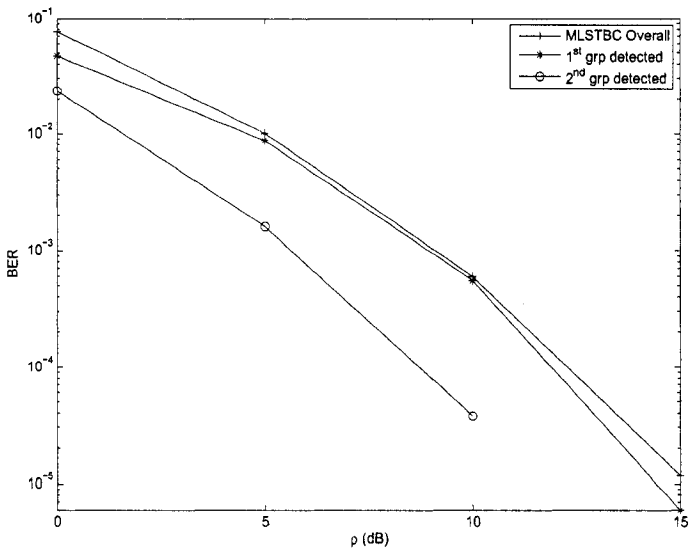

Figure 2.19: BER performance of MLSTBC with error propogation at each detection stage.

2.8 Chapter Summary

In this chapter we presented an overview of different STC schemes. STC is a coding technique intended for use with multiple transmit and receive antennas. Applying STC to MIMO systems maximizes the capacity of the MIMO wireless channel. Coding is accomplished in both spatial and temporal domains. This is done to establish correlation among signals coming from different antennas and signals coming at different times. There exists several variations to space-time codes, these includes STTCs, STBCs and LST codes.

STCs may be divided into two categories, those that provide transmit diversity gain and those that provide spatial multiplexing gain. The two main types of STC that achieve transmit diversity are STTCs and STBCs, while LST provides spatial multiplexing gain.

The main types of STC that provide transmit diversity gain are the STBC and the STTC. In STTC, a trellis code is distributed over the multiple transmit antennas and multiple time slots to provide transmit diversity and coding gain. The decoding complexity of STTC increases exponentially as a function of the diversity level and transmission rate for a given number of transmit antennas. STBC tackles the complexity problem encountered with STTC and presents a promising solution. STBC employs a block code in the form of a transmission matrix to solely provide to the system transmit diversity but at a much lower decoding complexity cost than in the STTC case. The Alamouti scheme is one of the simplest STC structures and is designed for two transmit antennas that could be further generalized to

more than two transmit antennas.

In this chapter we also explored the different types of LST (BLAST) schemes which include the D-BLAST, the V-BLAST, and finally the H-BLAST. Different detection techniques were also studied which are used in the detection process of LST schemes. Further, simulation results of the different LST architectures and different detection algorithms are also evaluated.

Chapter 3

A Low Complexity MMSE Detector for MLSTC Systems

3.1 Introduction

The MLSTC architecture was introduced in [20] by Tarokh et al, to provide an improved trade-off between spatial diversity and multiplexing gain. The MLSTC scheme merges coding concepts at the transmitter and signal array processing at the receiver. This scheme enhances the systems performance by augmenting the spatial diversity order and increasing the spatial multiplexing gain by adopting approaches of LST coding. In particular, the MLSTC scheme divides the transmit antennas into subgroups and each subgroup has its corresponding STC.

At the receiver, each individual STC is decoded using a linear processing technique that first suppresses the signals transmitted from the other subgroups by considering them as interferers. This detection algorithm is called the group interference cancellation (GIC) detector [20]. One of the constraints of this decoding scheme is the number of receive antennas where it is required that $N_r \geq N_t - n + 1$ in order to suppress the interference coming from the other groups, where n is the number of antennas in each group. In practice, it is not practical to implement many receive antennas on a mobile device. Other decoding schemes exist for V-BLAST systems but can not be applied directly to MLSTC. One very interesting V-BLAST decoding scheme was proposed in [24], and [25], which applies a MMSE-QRD based decoder. This scheme in contrast to other sub-optimal decoders shows notable system performance enhancement.

In this chapter, we extend the QRD-based MMSE decoder to decode a MLSTC system that will have reduced computational complexity, compared to the architecture introduced in [20]. The proposed decoder has been proven to enhance the overall performance of the

MLSTC architecture, while also benefiting from a lower complexity, the number of receive antennas necessary can also be relaxed. Further, in order for all groups, which can be viewed as individual users, to benefit from a similar performance, unequal power allocation strategy will be employed to the system.

3.2 System Model

The MLSTC system consists of K parallel STBC encoders independent from one another. Since we are dealing with STBC, we will refer from now on to our system as MLSTBC. Each encoder consists of n antennas and is refereed to as a group. The total number of transmit antennas N_t is equal to $K \cdot n$. The receiver has N_r receive antennas, the number of receive antennas must satisfy the condition $N_r \geq K$ and can thus be less than the number of transmit antennas. The MLSTBC system can be noted as (N_t, n, N_r). The system transmitter is shown in Figure 3.1.

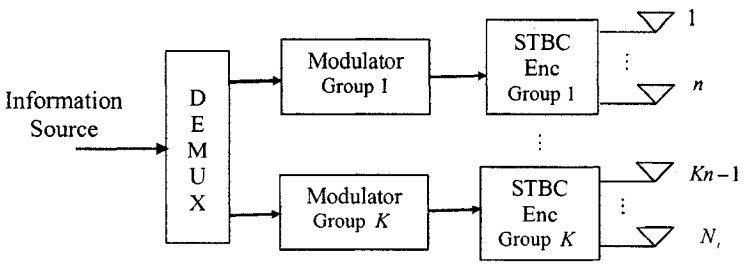

Figure 3.1: MLSTBC transmitter.

Let

$$\mathbf{X} = \begin{bmatrix} x_{1,1} & \cdots & x_{1,L} \\ \vdots & \ddots & \vdots \\ x_{N_t,1} & \cdots & x_{N_t,L} \end{bmatrix} \tag{3.1}$$

denote the $N_t \times L$ transmit signal matrix where L is the frame length. Each row represents the symbols transmitted by each transmit antenna.

In a MLSTBC system, the overall transmit signal can be described by stacking all the

signal matrices resulting from each layers' STBC encoder $\mathbf{G}_i(x)$ for $i = 1, 2, \ldots, K$ as

$$\mathbf{G}(x) = \begin{bmatrix} \mathbf{G}_1(x) \\ \mathbf{G}_2(x) \\ \vdots \\ \mathbf{G}_K(x) \end{bmatrix}. \tag{3.2}$$

For example we will examine a system model with two groups $K = 2$, where each group employs a STBC encoder with $n = 2$ transmit antennas, and with four receive antennas $N_r = 4$. The data stream is demultiplexed into K substreams (layers) and each layer is assigned to a group. Thus, for $L = 1$, $G(x)$ may be expressed as

$$\begin{aligned} \mathbf{G}(x) &= \begin{bmatrix} \mathbf{G}_1(x) \\ \mathbf{G}_2(x) \end{bmatrix} \\ &= \begin{bmatrix} x_{1,1} & -x_{2,1}^* \\ x_{2,1} & x_{1,1}^* \\ x_{3,1} & -x_{4,1}^* \\ x_{4,1} & x_{3,1}^* \end{bmatrix}. \end{aligned} \tag{3.3}$$

The received signal may be expressed as

$$\mathbf{Y} = \mathbf{H}\mathbf{G}(x) + \mathbf{N}, \tag{3.4}$$

where $\mathbf{H}$ is the fading coefficient matrix of size $N_r \times N_t$ with elements $h_{i,j}$ representing the fading gains between the jth transmit antenna and the ith receive antenna. These fading coefficients are assumed to be independent and $\mathcal{CN}(0, 1)$ distributed. The matrix $\mathbf{N}$ is composed of $\mathcal{CN}(0, N_0)$ distributed noise samples with a size of $N_r \times nL$.

3.3 Proposed MMSE-QRD MLSTC Decoder

It was demonstrated in [24] that we can incorporate the MMSE criterion into the QRD and further into the sorted QRD (SQRD). The use of MMSE-QRD/SQRD requires only a fraction of the computation compared to the BLAST detection algorithm proposed in [2]. The MMSE decoder gives better performance than the ZF decoder. That is because the MMSE detector minimizes the mean squared error linking the transmitted symbols and the

output of the linear detector. The ZF filter matrix is expressed as

$$\mathbf{G}_{ZF} = \mathbf{H}^{\dagger} = (\mathbf{H}^H\mathbf{H})^{-1}\mathbf{H}^H, \tag{3.5}$$

while the MMSE filter matrix is expressed as

$$\mathbf{G}_{MMSE} = (\mathbf{H}^H\mathbf{H} + \delta_n^2\mathbf{I}_{N_t})^{-1}\mathbf{H}^H, \tag{3.6}$$

where $\mathbf{A}^H$ is the conjugate transpose of matrix $\mathbf{A}$, $\delta_n^2 = N_0$ is the noise variance, and $\mathbf{I}_{N_t}$ is a $N_t \times N_t$ identity matrix.

In [24], the authors demonstrate that with the definition of a $(N_r + N_t) \times N_t$ extended channel matrix $\bar{\mathbf{H}}$ and a $(N_r + N_t) \times 1$ extended receive matrix $\bar{\mathbf{Y}}$, the MMSE filter matrix may be rewritten as

$$\mathbf{G}_{MMSE} = (\bar{\mathbf{H}}^H\bar{\mathbf{H}})^{-1}\bar{\mathbf{H}}^H, \tag{3.7}$$

where

$$\bar{\mathbf{H}} = \begin{bmatrix} \mathbf{H} \\ \delta_n\mathbf{I}_{N_t} \end{bmatrix} \text{ and } \bar{\mathbf{Y}} = \begin{bmatrix} \mathbf{Y} \\ \mathbf{0}_{N_t} \end{bmatrix}, \tag{3.8}$$

where $\mathbf{0}_{N_t}$ is a $N_t \times N_t$ zero matrix.

Comparing the filter matrix in (3.7) to that of the ZF filter matrix found in (3.5), we can now see the similarity. The only difference lies in the extended channel matrix. From this we can easily apply the QRD as follows

$$\bar{\mathbf{H}} = \begin{bmatrix} \mathbf{H} \\ \delta_n\mathbf{I}_{N_t} \end{bmatrix} = \mathbf{QR} = \begin{bmatrix} \mathbf{Q}_1 \\ \mathbf{Q}_2 \end{bmatrix}\mathbf{R} = \begin{bmatrix} \mathbf{Q}_1\mathbf{R} \\ \mathbf{Q}_2\mathbf{R} \end{bmatrix}, \tag{3.9}$$

where the matrix $\mathbf{Q}$ was divided into the $N_r n \times N_t$ matrix $\mathbf{Q}_1$, and the $N_t \times N_t$ matrix $\mathbf{Q}_2$.

The MMSE-QRD scheme cannot be directly applied to the MLSTBC system. It has to be modified to suit the MLSTBC scheme structure. To this end, we re-write the received matrix as

$$\mathbf{Z} = \mathbf{H}_{eq}\mathbf{X} + \mathbf{N}_{eq}, \tag{3.10}$$

where $\mathbf{H}_{eq}$ is the equivalent channel matrix of dimension $(N_r T) \times N_t$, and $\mathbf{N}_{eq}$ is the equivalent noise matrix. The transmitted signal is now represented in the matrix $\mathbf{X}$ as in (3.1).

For example if we are employing the Alamouti scheme and we have a $(4, 2, 4)$ MIMO

system then we have a total of 2 groups. We can then represent the channel matrix by

$$\mathbf{H} = \begin{bmatrix} h_{1,1} & h_{1,2} & h_{1,3} & h_{1,4} \\ h_{2,1} & h_{2,2} & h_{2,3} & h_{2,4} \\ h_{3,1} & h_{3,2} & h_{3,3} & h_{3,4} \\ h_{4,1} & h_{4,2} & h_{4,3} & h_{4,4} \end{bmatrix}.$$

The transmission matrix $\mathbf{G}(x)$ is composed of the two groups transmission matrices and is represented as in (3.3).

Thus the equivalent channel matrix $\mathbf{H}_{eq}$ for this case would be

$$\mathbf{H}_{eq} = \begin{bmatrix} h_{1,1} & h_{1,2} & h_{1,3} & h_{1,4} \\ h_{2,1} & h_{2,2} & h_{2,3} & h_{2,4} \\ h_{3,1} & h_{3,2} & h_{3,3} & h_{3,4} \\ h_{4,1} & h_{4,2} & h_{4,3} & h_{4,4} \\ h_{1,2}^* & -h_{1,1}^* & h_{1,4}^* & -h_{1,3}^* \\ h_{2,2}^* & -h_{2,1}^* & h_{2,4}^* & -h_{2,3}^* \\ h_{3,2}^* & -h_{3,1}^* & h_{3,4}^* & -h_{3,3}^* \\ h_{4,2}^* & -h_{4,1}^* & h_{4,4}^* & -h_{4,3}^* \end{bmatrix}. \tag{3.11}$$

We can now take the QRD of the equivalent channel matrix $\mathbf{H}_{eq}$ while successfully decoding each layer separately and holding their STBC orthogonal properties. We start by taking the QRD of the equivalent channel matrix in (3.11), but first we must extend the channel matrix as explained earlier, thus

$$\bar{\mathbf{H}}_{eq} = \begin{bmatrix} \mathbf{H}_{eq} \\ \delta_n \mathbf{I}_{N_t} \end{bmatrix}. \tag{3.12}$$

We continue by extending the received matrix $\mathbf{Z}$ found in (3.10) as follows

$$\bar{\mathbf{Z}} = \begin{bmatrix} \mathbf{Z} \\ \mathbf{0}_{N_t} \end{bmatrix}. \tag{3.13}$$

We then take the QRD of the extended channel matrix $\bar{\mathbf{H}}_{eq} = \mathbf{QR}$, where $\mathbf{Q}$ is an orthonormal column matrix of size $(N_t + N_r T) \times N_t$, and $\mathbf{R}$ is an upper triangular matrix. From knowing that

$$\mathbf{Q}^H \bar{\mathbf{H}}_{eq} = \mathbf{Q}_1^H \mathbf{H}_{eq} + \delta_n \mathbf{Q}_2^H \tag{3.14}$$

$$= \mathbf{Q}^H\mathbf{Q}\mathbf{R} \tag{3.15}$$

$$= \mathbf{R}, \tag{3.16}$$

holds, we should pre-multiply $\mathbf{Q}^H$ with the extended receive matrix $\bar{\mathbf{Z}}$, to obtain the decision statistics $\tilde{\mathbf{Z}}$ matrix of the transmitted signals as

$$\begin{aligned}\tilde{\mathbf{Z}} &= \mathbf{Q}^H\bar{\mathbf{Z}} \\ &= \mathbf{Q}_1^H\mathbf{Z} \\ &= \mathbf{R}\mathbf{X} - \delta_n^2\mathbf{R}^{-H}\mathbf{X} + \mathbf{Q}_1^H\mathbf{N}_{eq}.\end{aligned} \tag{3.17}$$

The second term of (3.17) represents residual interference that can not be removed by the successive interference cancellation process. Since $\mathbf{Q}$ is unitary, the statistical properties of the noise term $\mathbf{Q}_1^H\mathbf{N}_{eq}$ remain unaffected. The expansion of $\tilde{\mathbf{Z}}$ in its element form may be expressed as

$$\tilde{z}_{i,t} = r_{i,i}x_{i,t} + \sum_{k=i+1}^{N_t} r_{i,k}x_{k,t} + \tilde{n}_{i,t}, \tag{3.18}$$

where $\tilde{n}_{i,t}$ is the corresponding noise term. The first part of this expansion represents the desired symbol followed by the second part which is the interference. The term $r_{i,i}$ is the element from the $\mathbf{R}$ matrix found at the ith column and ith row. To obtain the desired symbol we must cancel the interference part, thus once a layer is detected, its interference contribution is calculated and subtracted from the received signal as

$$\tilde{z}_{i,t} = \tilde{z}_{i,t} - \sum_{k=i+1}^{N_t} r_{i,k}\hat{x}_{k,t}. \tag{3.19}$$

For an unordered system, the first layer detected is N_t due to the upper triangular properties of the matrix $\mathbf{R}$, which is made clear from examining (3.18). The $(N_t - 1)$th layer is subsequently detected. This procedure continues until the first layer is detected last.

The order of the detection process is a crucial factor in the error probability performance. It is best to choose and detect the layer with the largest post detection SNR first. Thus, we place the weaker layers later in the detection process, since the overall system performance is limited by the performance of the first detected layer.

It is quite simple to achieve this strategy. We must first order the channel matrix $\mathbf{H}_{eq}$ with columns having smallest norms first to highest values of column norms. Thus, we can

find the order of detection k for $i = 1, \ldots, N_t$ to be

$$k_i = \arg \min_{l=i, \ldots, N_t} \|h_l\|^2,$$

where h_l represents the lth column of the channel matrix $\mathbf{H}_{eq}$, and $\|\cdot\|$ represents the norm operation. Once the sorted channel matrix $\mathbf{H}_{eq}$ is found, we apply the QRD to the extended channel matrix $\bar{\mathbf{H}}_{eq}$ to obtain new $\mathbf{Q}$ and $\mathbf{R}$ matrices. The new $\mathbf{R}$ matrix will have a property that r_{N_t,N_t} will be maximized over the entire potential combination of the columns of the channel matrix $\mathbf{H}$, followed by r_{N_t-1,N_t-1}, until we reach $r_{1,1}$, which will have the smallest value.

3.4 Diversity Order of MMSE-QRD Detector Used in a MLSTBC System

The first group detected in the MLSTBC scheme presented in [20], achieves a diversity gain of $n_1 \times (n_1 + N_r - N_t)$, where n_k are the antennas from the kth STBC encoder. After decoding the first group and subtracting its interference from the received signal, the second group can be detected, which achieves a diversity gain of $n_2 \times (n_2 + n_1 + N_r - N_t)$. Thus for the kth detected group, a diversity gain of [20]

$$n_k \times (n_1 + n_2 + \cdots + n_k + N_r - N_t), \tag{3.20}$$

is achieved.

We know that the received signal for the MLSTBC system using the MMSE-QRD detector is

$$\mathbf{Z} = \mathbf{H}_{eq}\mathbf{X} + \mathbf{N}_{eq},$$

where $\mathbf{H}_{eq}$ is the equivalent channel matrix of dimension $(N_r T) \times N_t$, and $\mathbf{N}_{eq}$ is the equivalent noise matrix.

If we look at the received signal in more detail but ignore the noise term for now we have for a $(4, 2, 2)$ system

$$\mathbf{Z} = \begin{bmatrix} h_{1,1} & h_{1,2} & h_{1,3} & h_{1,4} \\ h_{2,1} & h_{2,2} & h_{2,3} & h_{2,4} \\ h_{1,2}^* & -h_{1,1}^* & h_{1,4}^* & -h_{1,3}^* \\ h_{2,2}^* & -h_{2,1}^* & h_{2,4}^* & -h_{2,3}^* \end{bmatrix} \begin{bmatrix} x_{1,1} & \cdots & x_{1,L} \\ \vdots & \ddots & \vdots \\ x_{4,1} & \cdots & x_{4,L} \end{bmatrix}$$

$$= \begin{bmatrix} z_{1,1} & \cdots & z_{1,L} \\ \vdots & \ddots & \vdots \\ z_{4,1} & \cdots & z_{4,L} \end{bmatrix}$$

After following the procedure explained in the previous section, we arrive at the decision statistics

$$\tilde{\mathbf{Z}} = \mathbf{RX} - \delta_n^2 \left(\mathbf{R}^{-1}\right)^H \mathbf{X} + \mathbf{Q}_1^H \mathbf{N}_{eq}.$$

By expanding the first term we arrive at

$$\mathbf{RX} = \begin{bmatrix} r_{1,1} & r_{1,2} & r_{1,3} & r_{1,4} \\ 0 & r_{2,2} & r_{2,3} & r_{2,4} \\ 0 & 0 & r_{3,3} & r_{3,4} \\ 0 & 0 & 0 & r_{4,4} \end{bmatrix} \begin{bmatrix} x_{1,1} & \cdots & x_{1,L} \\ \vdots & \ddots & \vdots \\ x_{4,1} & \cdots & x_{4,L} \end{bmatrix}.$$

From this we can observe that the receive diversity using the MMSE-QRD algorithm should be the same concept as in V-BLAST. Thus the receive diversity is

$$d_{receive} = N_r - k + 1,$$

where k is the layer that is being detected and not the stream as in the V-BLAST case where each stream was a layer.

For example for a system with four transmit antennas and two receive antennas $(4, 2, 2)$ the diversity for the first group detected (which is the second layer) will be

$$d_1 = 2 \times (2 - 2 + 1) = 2 \times 1,$$

and the second group detected (which is the first layer)

$$d_2 = 2 \times (2 - 1 + 1) = 2 \times 2.$$

Until now this result is consistent with the GIC diversity results for MLSTBC, however let us examine for a different number of receive antennas. If we have a system with four transmit antennas and three receive antennas $(4, 2, 4)$ the diversity for the first group detected (which is the second layer) will be

$$d_1 = 2 \times (4 - 2 + 1) = 2 \times 3 = 6,$$

and the second group detected (which is the first layer)

$$d_2 = 2 \times (4 - 1 + 1) = 2 \times 4 = 8.$$

Here we can note where the difference lies. In the GIC detector case, the diversity for a $(4, 2, 4)$ system would have been $2 \times 2 = 4$, for the first group and $2 \times 4 = 8$ for the second group. Hence we see an exceptional increase in diversity using the MMSE-QRD detector in the first layer detected, which is a crucial milestone for the performance of the overall system.

3.4.1 Analysis

The simplified steps to acquire the $\mathbf{R}$ matrix in the QRD are

$\mathbf{Q} = \mathbf{H}$

for $k = i + 1, \ldots, N_t$

$r_{i,k} = \mathbf{q}_i^H \mathbf{q}_k$

end

$r_{i,i} = \|\mathbf{q}_i\|^2$, where $r_{i,k}$ is the (i,k)th element of the matrix $\mathbf{R}$, and $\mathbf{q}_k$ is the kth column of the matrix $\mathbf{Q}$.

If we take a $N_t \times N_r$ MLSTBC system, the equivalent channel matrix $\mathbf{H}_{eq}$ will be

$$\mathbf{H}_{eq} = \begin{bmatrix} h_{1,1} & h_{1,2} & \cdots & h_{1,N_t-1} & h_{1,N_t} \\ h_{2,1} & h_{2,2} & \cdots & h_{2,N_t-1} & h_{2,N_t} \\ \vdots & \vdots & \ddots & \vdots & \vdots \\ h_{N_r,1} & h_{N_r,2} & \cdots & h_{N_r,N_t-1} & h_{N_r,N_t} \\ h_{1,2}^* & -h_{1,1}^* & \cdots & h_{1,N_t}^* & -h_{1,N_t-1}^* \\ \vdots & \vdots & \ddots & \vdots & \vdots \\ h_{N_r,2}^* & -h_{N_r,1}^* & \cdots & h_{N_r,N_t}^* & -h_{N_r,N_t-1}^* \end{bmatrix}.$$

Thus following the steps of procuring the $\mathbf{R}$ matrix we will obtain the following

$$\begin{aligned} r_{1,1} &= \sqrt{|h_{1,1}|^2 + |h_{2,1}|^2 + |h_{N_r,1}|^2 + \ldots + |h_{1,2}^*|^2 + \ldots + |h_{N_r,2}^*|^2} \\ r_{2,2} &= \sqrt{|h_{1,2}|^2 + |h_{2,2}|^2 + |h_{N_r,2}|^2 + \ldots + |-h_{1,1}^*|^2 + \ldots + |-h_{N_r,1}^*|^2} \\ &\therefore \quad r_{1,1} = r_{2,2} \end{aligned} \tag{3.21}$$

$$
\begin{aligned}
r_{N_t-1,N_t-1} &= \sqrt{|h_{1,N_t-1}|^2 + |h_{2,N_t-1}|^2 + \ldots + |h^*_{1,N_t}|^2 + \ldots + |h^*_{N_r,N_t}|^2} \\
r_{N_t,N_t} &= \sqrt{|h_{1,N_t}|^2 + |h_{2,N_t}|^2 + \ldots + |-h^*_{1,N_t-1}|^2 + \ldots + |-h^*_{N_r,N_t-1}|^2} \\
&\therefore \; r_{N_t-1,N_t-1} = r_{N_t,N_t} \qquad (3.22)
\end{aligned}
$$

All of the diagonal of the $\mathbf{R}$ matrix will be identical in pairs as in (3.21) and (3.22). For the upper non-diagonal elements of the matrix, the columns that contain the same elements but in different order are orthogonal to each other. Thus, when they are multiplied will produce a value of zero. For example:

$$
\begin{aligned}
r_{1,2} &= \mathbf{q}_1^H \mathbf{q}_2 = 0, \\
r_{N_t-1,N_t} &= \mathbf{q}_{N_t-1}^H \mathbf{q}_{N_t} = 0.
\end{aligned}
$$

The remaining upper non-diagonal entries of the matrix will be result in complex conjugate of each other. For example:

$$
\begin{aligned}
r_{1,N_t-1} &= \mathbf{q}_1^H \mathbf{q}_{N_t-1}, \\
r_{1,N_t} &= \mathbf{q}_1^H \mathbf{q}_{N_t}, \\
r_{2,N_t-1} &= \mathbf{q}_2^H \mathbf{q}_{N_t-1}, \\
r_{2,N_t} &= \mathbf{q}_2^H \mathbf{q}_{N_t}.
\end{aligned}
$$

From these results we can conclude that $r_{2,N_t-1} = -r^*_{1,N_t}$ and $r_{2,N_t} = r^*_{1,N_t-1}$. We can thus re-write the $\mathbf{R}$ matrix to be something like this

$$
\mathbf{R} = \begin{bmatrix}
r_{1,1} & r_{1,2} & \cdots & r_{1,N_t-1} & r_{1,N_t} \\
0 & r_{2,2} & \cdots & r_{2,N_t-1} & r_{2,N_t} \\
0 & 0 & \ddots & \vdots & \vdots \\
0 & 0 & 0 & r_{N_t-1,N_t-1} & r_{N_t-1,N_t} \\
0 & 0 & 0 & 0 & r_{N_t,N_t}
\end{bmatrix} = \begin{bmatrix}
r_{1,1} & 0 & \cdots & r_{1,N_t-1} & r_{1,N_t} \\
0 & r_{1,1} & \cdots & -r^*_{1,N_t} & r^*_{1,N_t-1} \\
0 & 0 & \ddots & \vdots & \vdots \\
0 & 0 & 0 & r_{N_t-1,N_t-1} & 0 \\
0 & 0 & 0 & 0 & r_{N_t-1,N_t-1}
\end{bmatrix}.
$$

From this, it is clear that the first two streams (layer 1) will experience the same diversity, and the last two streams (layer K) will also have the same diversity as each other since the number of interferers in the streams are equal. From the "new" $\mathbf{R}$ matrix, there is an interesting observation to note, which is that at the first substream, only 1 layer (not to be confused with substream) is being suppressed since the second substream has identical channel properties, and the two subsequent substreams have similar substreams. This is

the reason for an example of a $(4, 2, 4)$ system the diversity of the first two substreams will have diversity of 3, since there is physically only one suppression and not two. For the two subsequent substreams there is no suppression to be done, since the two constitute a layer and have same channel properties (due to orthogonal nature of transmission matrix).

We come to the conclusion that the overall diversity order of the MLSTBC scheme with the MMSE-QRD detector is

$$d_{MLSTBC-MMSE_{QRD}} = n \times (N_r - K + 1),$$

assuming all the subgroups apply the same number of transmit antennas.

3.5 Computational Complexity

With any algorithm, it is important to consider its cost. We can do this by counting the floating point operations (flops). In this section we investigate the computational complexity of the proposed MMSE-QRD scheme for MLSTBC system and compare it to that of the GIC scheme proposed in [20]. In our derivation of the number of flops, we assume that all multiplications, division, additions, and subtractions are counted as one flop. The number of flops of these algorithms are derived in terms of their system variables N_t , N_r and n.

The main difference in the algorithm of the MMSE-QRD MLSTBC and the GIC lies in the suppression step. For the MMSE-QRD, the QRD of the extended channel matrix is taken. This step is only done once for all the layers to be decoded. For the GIC scheme, one must take the pseudo inverse of the group channel matrix to be first suppressed, then take the null space of this matrix. This sequence of action is done $\left(\frac{N_t}{n} - 1\right)$ times in the scheme. Thus it was found that the MMSE-QRD scheme requires

$$f_{MMSE-QRD} = 2N_t^3 + 2N_t^2 N_r - \frac{5}{2}N_t^2 - 2N_t N_r + \frac{N_t}{2}, \tag{3.23}$$

and that the GIC scheme requires

$$f_{GIC} = \left(\frac{N_t}{n} - 1\right) \cdot \begin{array}{c}[2n^3 - 3n^2 + n + N_r(3n^2 + N_t^2 - N_t + \\ \frac{2}{3}N_r^2 + \frac{3}{2}N_r - \frac{7}{6})]\end{array}. \tag{3.24}$$

A more detailed look at the flop count can be seen in Table 3.1 for the MMSE-QRD detector and in Table 3.2 for the GIC, where the first row presents the number of multiplications, the second row represents the number of additions, and finally the third row represents the

total number of flops for each detector.

Table 3.1: MMSE-QRD Computational Complexity Breadk-Down

	MMSE-QRD
No. of Mult (flops)	$N_r\left(N_t^2 - N_t\right) + N_t^3 - N_t^2$
No. of Add (flops)	$N_t^2 N_r + N_t^3 - N_t N_r - \frac{3}{2}N_t^2 + \frac{N_t}{2}$
Total	$2N_t^2 N_r + 2N_t^3 - 2N_t N_r - \frac{5}{2}N_t^2 + \frac{N_t}{2}$

Table 3.2: GIC Computational Complexity Breadk-Down

	GIC
No. of Mult (flops)	$\left(\frac{N_t}{n} - 1\right)\left(\frac{N_r^3}{3} + N_r^2 + n^3 + 2n^2 N_r - \frac{N_r}{3}\right)$
No. of Add (flops)	$\left(\frac{N_t}{n} - 1\right)\left\|n^3 + n - 3n^2 + N_r\left(\frac{N_r^2}{3} + N_t^2 + \frac{N_r}{2} + n^2 - N_t - \frac{5}{6}\right)\right.$
Total	$\left(\frac{N_t}{n} - 1\right)\left\|2n^3 + n - 3n^2 + N_r\left(\frac{2N_r^2}{3} + N_t^2 + \frac{3N_r}{2} + 3n^2 - N_t - \frac{7}{6}\right)\right.$

In Figure 3.2 we demonstrate the difference in the computational complexity between the two algorithms for a system with varying transmit and receive antennas that are equal in number, while using the Alamouti scheme, thus $n = 2$. We can observe from the figure that the MMSE-QRD algorithm exhibits lower computational complexity than the GIC algorithm especially as the number of antennas increases.

3.6 Transmit Power Allocation

In a multiuser system, we desire all users to benefit from somewhat the same performance. In the MLSTBC system, a diversity order for an earlier detection group is less than that for a later one. Thus, early detected groups may limit the overall performance. In the previous section, the SQRD algorithm was implemented to compensate for low diversity orders of early detection groups. Yet, this scheme may not adequately balance for low diversity orders in early detection groups. Thus transmit power allocation (PA) may suggest additional enhancement in the performance of early detection groups and thus improving the overall performance, while additionally making the performance gap between different groups smaller. Consequently, the transmitter should allocate the available transmit power between the different antennas in an unequal way. In [26], and [27] transmit power allocation algorithm was defined for the V-BLAST scheme. The power to be allocated to the different groups should be based on their diversity gains as mentioned in [20]. For an ordered scheme, the ordering already brings the gap between the two groups closer, so a less dramatic PA strategy is needed.

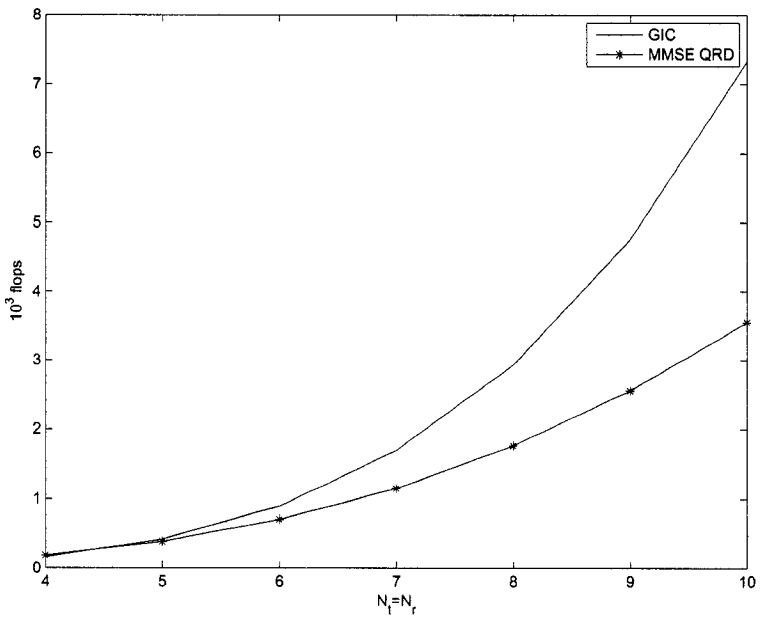

Figure 3.2: Number of flops for MMSE-QRD and GIC scheme

3.7 Simulation Results

In our simulations, we use the system model for the MLSTBC depicted in Figure 2.17. The proposed MMSE-QRD/SQRD detectors described in Section 3.3 as well as the GIC detector were used in the simulations. The channel fading coefficients remained unvarying over a block of length $L = 100$ consecutive symbols and vary independently from one block to another. BPSK modulation was applied to the system.

In Figure 3.3, we plot the overall BER results for a $(4, 2, 4)$ MLSTBC system with error propagation included in the various detection stages for three types of detectors. The detectors applied for this Figure are the GIC, MMSE-QRD, and the MMSE-SQRD detectors. Observing the simulation results from Figure 3.3, a remarkable performance improvement is shown between the proposed algorithm and GIC. The MMSE-SQRD algorithm further enhances the performance as demonstrated in the simulation results. The simulation results demonstrate the diversity gain attained by the new MMSE-QRD detector. For this $(4, 2, 4)$ system, the GIC detector attains an overall diversity gain of $n \times (N_r - N_t + n) = 2 \times 2 = 4$, while the MMSE-QRD detector achieves a diversity gain of $n \times (N_r - n + 1) = 2 \times 3 = 6$. The ordering of the detection stages in the MMSE-SQRD detector further enhances the performance of the MLSTBC scheme by $\sim 1.5dB$.

In Figure 3.4 we demonstrate the simulation results obtained for the first detected layer

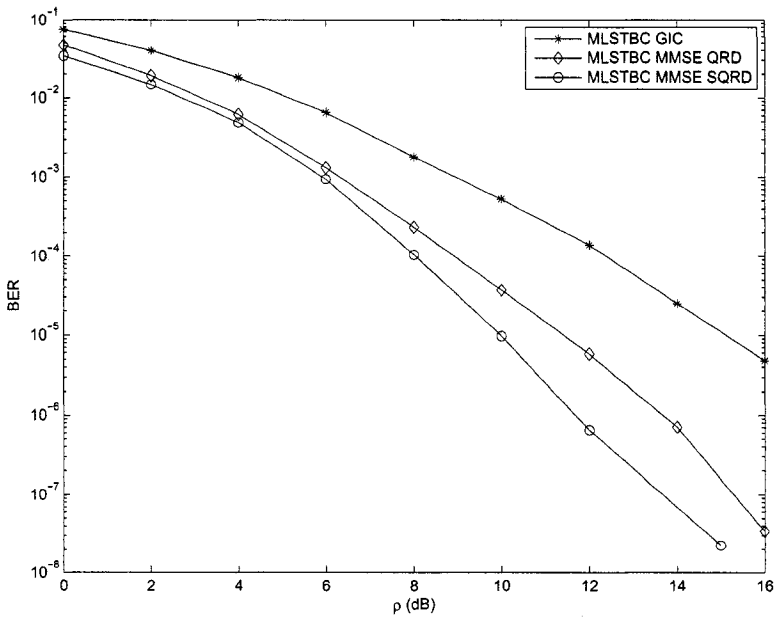

Figure 3.3: BER performance of MLSTBC system with the proposed decoder and the GIC decoder.

of a $(4, 2, 2)$, $(4, 2, 3)$, and $(4, 2, 4)$ MLSTBC scheme applying the MMSE-QRD detector and using the "genie" algorithm. Also plotted in the same figure are the theoretical results obtained from the interference free bound (IFB) equation with diversity indicated in the legend given by [23]

$$P_b \approx \binom{2n(N_r - n + 1) - 1}{n(N_r - n + 1)} (4\rho)^{-n(N_r - n + 1)},$$

where $\rho = \frac{E_b}{N_t N_0}$.

The simulation results from Figure 3.4 further justify the analysis for the diversity order of the first detected layer. It also demonstrates the capability of the MMSE-QRD MLSTC detector to detect with smaller number of receive antennas, specifically with $N_r \geq K$.

We plot in Figure 3.5 the BER performance of the first and second layer detected for a $(4, 2, 4)$ MLSTBC system using MMSE-QRD detector and using the "genie" method, thus perfect estimation of previous layers is assumed. From the figure we can deduce that the first detected layer of the MLSTBC scheme determines the overall performance of the MLSTBC scheme. We can also observe that employing the MMSE-QRD detector, the first detected layer has increased performance than that of the MLSTBC scheme employing the GIC detector.

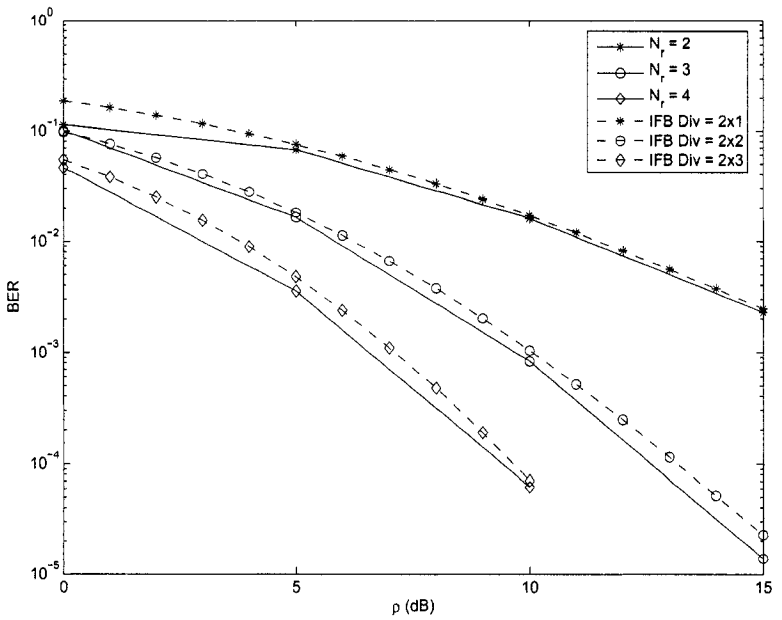

Figure 3.4: BER performance results of the MLSTBC system with the proposed MMSE-QRD detector applying different number of receive antennas.

In Figure 3.6 we show a comparison of the performance results between the different detection groups at different detection stages applying the PA technique. We see that when ordering and PA is placed in the system, the first detected group's performance is improved. The second detected group's performance is brought closer to that of the first one, thus multiusers will benefit from the same performance. The PA applied to this system takes in consideration the ordering scheme used and the diversity orders of the groups. We have allocated 53% of the power to the first group detected, and the remaining 47% to the second group.

3.8 Chapter Summary

In this chapter, we analyzed the performance of the proposed MMSE-QRD detector in conjunction with the MLSTBC architecture. Our analysis showed that the MMSE-QRD detector increased the diversity gain of the system. Specifically the diversity gain was found to be $n \times (N_r - k + 1)$, where k is the kth detection sub-group. It was also demonstrated that added performance was reached with the sorted algorithm (MMSE-SQRD) and that by applying the PA strategy, the performance gap between the different layers of the MLSTBC architecture can be brought closer, which is an important feature for multiuser systems. It was also

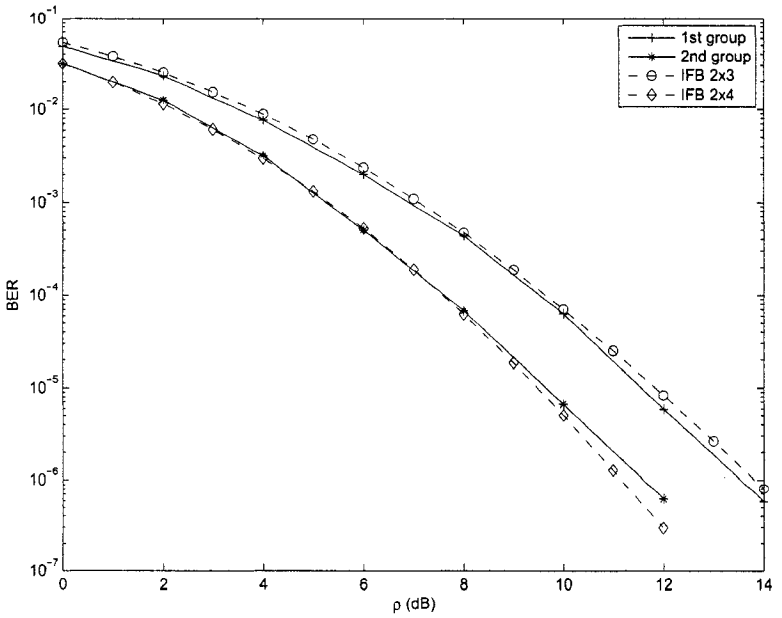

Figure 3.5: BER performance of 1st and 2nd detected groups of MLSTBC using the MMSE-QRD detector with the "genie" method.

found that the proposed MMSE-QRD detector has reduced computational complexity compared to the GIC detector previously applied to the MLSTBC architecture. Additionally the MMSE-QRD detector has the advantage of being able to detect with a reduced number of receive antennas, where the restrictions on the receive antennas must satisfy $N_r \geq K$, while for the GIC detector the restriction on the number of receive antennas is $N_r \geq N_t - n + 1$.

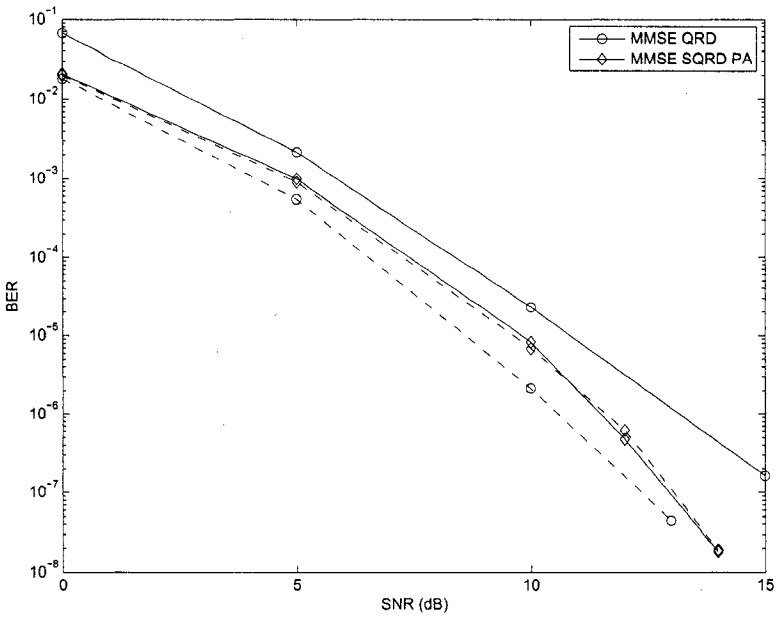

Figure 3.6: Comparison BER of a $(4, 2, 4)$ MLSTBC system with ordering and proposed power allocation, first group detected (contionus line) and second group detected (dashed line)

Chapter 4

Multilayered Space-Time Coding for Frequency Selective Fading Channels

In a wideband wireless communication system, there is the existence of a multipath channel. Consequently, intersymbol interference (ISI) is subjected to the received signal. At high data rates, there is typically significant deterioration of the system's error rate performance [28]. Space-frequency-time (SFT) coding for OFDM applies spatial coding across multiple antennas, frequency coding across OFDM subcarriers and temporal coding across consecutive OFDM symbols. The initial SFT coding analysis was completed by [29] where they modified Tarokh's STC [5] to work with OFDM technology. Nonetheless, these codes are intended for quasi-static fading channels. Consequently, they are not optimized for frequency selective channels and do not take advantage from the available frequency diversity.

In this chapter, we study the performance results of a MLSTBC-OFDM system. Specifically, we examine the combination of MLSTC schemes with OFDM in order to combat the challenges posed by a frequency selective channel. We also propose a multilayered SFT OFDM scheme that employs the Alamouti algorithm at each subgroup and call it MLSFTBC-OFDM.

4.1 Multipath Channel

A critical complication in many wireless communication systems is the existence of a multipath channel. In a multipath channel environment, the transmitted signal reflects off from assorted objects. Consequently, multiple delayed versions of the transmitted signal emerge at the receiver. The multiple versions of the signal result in the received signal to be distorted mainly caused by intersymbol interference (ISI). At high data rates, there is typically

significant deterioration of the system's error rate performance [28].

The channel impulse response in the time domain is modeled as a tapped-delay line. Thus, for a frequency selective channel, the impulse response between the ith transmit and jth receive antenna is given by [19]

$$h_{j,i}(t;\tau) = \sum_{l=1}^{p} h_{j,i}^{t,l}\delta(\tau - \tau_l), \tag{4.1}$$

where p is the number of multipaths, τ_l is the time delay of the lth path and $h_{j,i}^{t,l}$ is the complex amplitude of the lth path.

In order to combat the effects of ISI, channel equalization techniques can be used to suppress the reflections caused by the channel. To execute this procedure, the channel impulse response must be estimated. However, equalization is relatively complex for MIMO channels. Additionally, many channel realization may not be equalizable.

Nonetheless, there exists a superior method towards transmitting data over a multipath channel. Instead of trying to cancel the effects of the channel's reflections, OFDM modems can be used, which employ a set of harmonically connected carriers in order to transmit information symbols in parallel over the channel. In a single carrier system, the data rate is R symbols/second contrary to an OFDM system, which has N_{FFT} subcarriers, each with a data rate of R/N_{FFT} symbols/second. This permits us to design a system sustaining high data rates, while preserving symbol durations much longer than the channel's memory, thus preventing the need for channel equalization. MIMO-OFDM systems, are broadly believed to be the choice of the technology for 4G wireless communication systems [30]-[35].

4.2 OFDM

The use of orthogonal subcarriers permits subcarriers' spectra to overlap, thus increasing spectral efficiency. Since OFDM takes advantage of orthogonal subcarriers, it is achievable to retrieve the individual subcarriers' signals regardless of their overlapping spectrums. Orthogonality can be viewed mathematically by the dot product. If the dot product of two distinct signals is equal to zero, these signals are said to be orthogonal to each other. Recall from signals and systems theory that the sinusoids of the DFT form an orthogonal basis set, and a signal in the vector space of the DFT can be represented as a linear combination of the orthogonal sinusoids. This transform is used at the OFDM transmitter to map an input signal onto a set of orthogonal subcarriers. The orthogonal and uncorrelated nature of the

subcarriers is exploited in OFDM with powerful results. Each subcarrier carries one bit of information (N_{FFT} bits in total for a N_{FFT} subcarrier OFDM symbol) by its presence or absence in the output spectrum [36]. The frequency of each subcarrier is selected to form an orthogonal signal set, and these frequencies are known at the receiver [33].

In practice, OFDM systems are implemented using a combination of fast Fourier Transform (FFT) and inverse FFT (IFFT), blocks that are mathematically equivalent version of the DFT and IDFT respectively, but more efficient to implement.

The system model of an OFDM scheme is shown in Figure 4.1. The incoming message is converted from a serial message into N_{FFT} parallel symbols, which enters the IFFT block. A cyclic prefix is then added to help combat the frequency selective channel. The cyclic prefix is basically a copy of the last p samples of the OFDM symbol. Hence, the total length of the transmitted OFDM symbol is $N_{FFT}+p$. The cyclic prefix length should be greater or equal to the length of the number of channel paths p. The signal is then transmitted through a frequency selective channel. At the receiver, the cyclic prefix is removed since it contains redundant information, and the signal is passed through a FFT block. OFDM with long enough cyclic prefix transforms the frequency selective channel into N_{FFT} independent flat fading subchannels [19], [34].

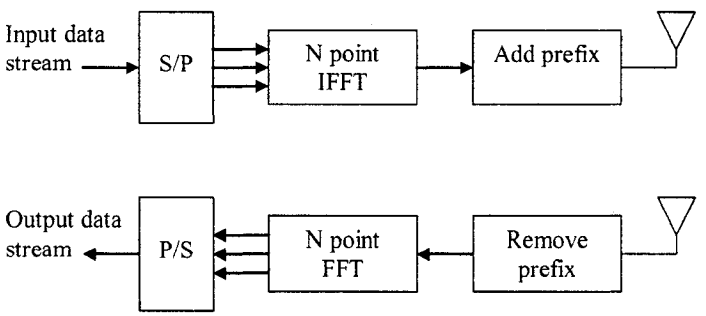

Figure 4.1: OFDM system model.

If we were to consider a SISO system in a frequency selective environment for the purpose of explanation, the received signal vector is

$$\mathbf{y} = \mathbf{h}X,$$

where $\mathbf{h}$ is the channel coefficient and X is the transmitted symbol.

Then the FFT of $\mathbf{y}$ is equal to the product of the FFTs of $\mathbf{h}$ and X, that is

$$\mathbf{Fy} = \mathbf{FhF}X,$$

where $\mathbf{F}$ is the DFT matrix whose (i,j)th entry is

$$f(i,j) = \frac{1}{\sqrt{N_{FFT}}} \exp\left(\frac{-j2\pi(i-1)(j-1)}{N_{FFT}}\right). \tag{4.2}$$

From matrix properties and manipulation, we can show that

$$\mathbf{FhF}X = \mathbf{FH}X = \mathbf{FHF}^H\mathbf{F}X,$$

Hence, $\mathbf{FHF}^H$ is a diagonal matrix whose jth diagonal entry is the jth N_{FFT}-point FFT coefficient of the channel vector $\mathbf{h}$, i.e.

$$\mathbf{\Lambda} = \mathbf{FHF}^H.$$

Now we have the Fourier transform of the received signal as

$$\mathbf{y}' = \mathbf{Fy} = \mathbf{FH}X = \mathbf{\Lambda F}X = \mathbf{\Lambda}x'.$$

That is, a frequency selective channel has been transformed into N_{FFT} parallel independent subchannels. Alternatively, we can view x' as a time domain signal, the original constant dispersive channel has now been transformed into a flat fading channel.

Following (4.1), let us indicate T_f as the time interval of each OFDM frame and Δf as the length of the difference between the OFDM subcarriers. This relationship is

$$\begin{aligned} T_f &= N_{FFT}T_s, \\ T_s &= \frac{1}{W} = \frac{1}{N_{FFT}\Delta f}, \end{aligned}$$

where W is the sampling rate at the receiver in Hz. The delay of the lth path presented in (4.1) can be expressed as

$$\tau_l = s_l T_s = \frac{s_l}{N_{FFT}\Delta f},$$

where s_l is an integer. Thus by performing the Fourier transform of the multipath channel response found in (4.1), we can obtain the channel frequency response at time t for the kth

subcarrier as [19]

$$\begin{aligned} H_{j,i}^{k} &\triangleq H_{j,i}(tT_f, k\Delta f) \\ &= \int_{-\infty}^{+\infty} h_{j,i}(tT_f, \tau) e^{-j2\pi k\Delta f \tau} d\tau \\ &= \sum_{l=1}^{p} h_{j,i}(tT_f, n_l T_s) e^{-j2\pi k s_l / N_{FFT}} \\ &= \sum_{l=1}^{p} h_{j,i}(t, n_l) e^{-j2\pi k s_l / N_{FFT}}. \end{aligned} \tag{4.3}$$

If we let

$$\mathbf{h}_{j,i}^{t} = \begin{bmatrix} h_{j,i}^{t,1} & h_{j,i}^{t,2} & \cdots & h_{j,i}^{t,p} \end{bmatrix}^H,$$

and

$$\mathbf{w}_k = \begin{bmatrix} e^{-j2\pi k s_1 / N_{FFT}} & e^{-j2\pi k s_2 / N_{FFT}} & \cdots & e^{-j2\pi k s_p / N_{FFT}} \end{bmatrix}^T,$$

equation (4.3) can be re-expressed as

$$H_{j,i}^{k} = \left(\mathbf{h}_{j,i}^{t}\right)^H \cdot \mathbf{w}_k,$$

where the channel frequency response $H_{j,i}^{k}$ is the digital Fourier transform of the channel impulse response $\mathbf{h}_{j,i}^{t}$ and $\mathbf{w}_k$, is a vector that performs the transform for the kth OFDM subcarrier, $k = 1, 2, \ldots, N_{FFT}$.

The advantages of using OFDM include high spectrum efficiency, robustness against multipath interference, and simplicity in filtering out noise. Furthermore, the upstream and downstream speeds can be changed by assigning added or less carriers for each case.

The opportunity to combine STC schemes with OFDM technology will allow for a MIMO system that will be effective against a wideband channel and have the various benefits of MIMO systems thus producing a reliable signal quality with the possibility of transmitting data at very high rates.

4.3 Multilayered Space-Time Coded OFDM Systems

In this section, we provide an overview of the combination of MLSTC schemes with OFDM in order to combat the challenges posed by a frequency selective channel. Specifically, we evaluate and compare the performance of MLSTBC-OFDM system using the MMSE-QRD

detector. In [37], [38], [39], [40], and [41] it was demonstrated that the V-BLAST and MLSTC schemes respectfully, can be successfully concatenated with OFDM to combat the frequency selective channel.

4.3.1 System Model of MLSTBC-OFDM

The MIMO frequency selective channel is assumed to be constant over the transmission of N_t OFDM symbols. At each time t, a transmission matrix of size $N_t \times L$ is transmitted where L is assumed to be equal to the number of OFDM subcarriers for simplicity, thus $L = N_{FFT}$. Therefore the transmission matrix at time t is given by

$$\mathbf{X} = \begin{bmatrix} x_{1,1} & x_{1,2} & \cdots & x_{1,L} \\ x_{2,1} & x_{2,2} & \cdots & x_{2,L} \\ \vdots & \ddots & \cdots & \vdots \\ x_{N_t,1} & x_{N_t,2} & \cdots & x_{N_t,L} \end{bmatrix}, \tag{4.4}$$

where the ith row is the data stream transmitted by the ith transmit antenna. Symbols $x_{i,1}, x_{i,2}, \ldots, x_{i,L}$ are OFDM modulated on N_{FFT} different OFDM subcarriers and transmitted from the ith transmit antenna simultaneously during one OFDM frame, where $x_{i,k}$ is sent on the kth OFDM subcarrier.

At the receiver the received signal at time t is

$$\mathbf{Y} = \mathbf{HX} + \mathbf{N},$$

where $\mathbf{X}$ is the transmission matrix as defined in (4.4), and $\mathbf{N}$ is a complex AWGN matrix of all subcarriers of zero mean and variance $N_0/2$ per dimension. $\mathbf{H}$ may be expressed as

$$\mathbf{H} = \begin{bmatrix} \mathbf{h}_{1,1} & \mathbf{h}_{1,2} & \cdots & \mathbf{h}_{1,N_t} \\ \mathbf{h}_{2,1} & \mathbf{h}_{2,2} & \cdots & \mathbf{h}_{2,N_t} \\ \vdots & \ddots & \cdots & \vdots \\ \mathbf{h}_{N_r,1} & \mathbf{h}_{N_r,2} & \cdots & \mathbf{h}_{N_r,N_t} \end{bmatrix},$$

where $\mathbf{h}_{j,i}$ is the OFDM channel vector in the frequency domain between the ith transmit antenna and jth receive antenna at time t and is a $N_{FFT} \times 1$ vector as

$$\mathbf{h}_{j,i} = \begin{bmatrix} H_{j,i}^1 & H_{j,i}^2 & \cdots & H_{j,i}^{N_{FFT}} \end{bmatrix},$$

where $H_{j,i}^{k}$ is the channel frequency response for the path between the ith transmit antenna and jth receive antenna on the kth OFDM subcarrier. The transmitter and decoder structure of the MLSTBC-OFDM system is shown in Figure 4.2 and 4.3, respectfully.

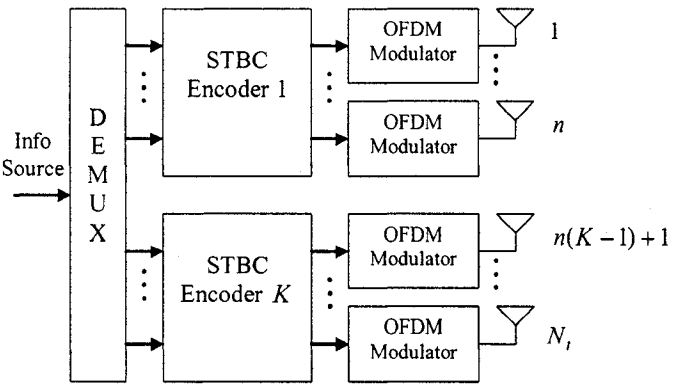

Figure 4.2: MLSTBC-OFDM transmitter structure.

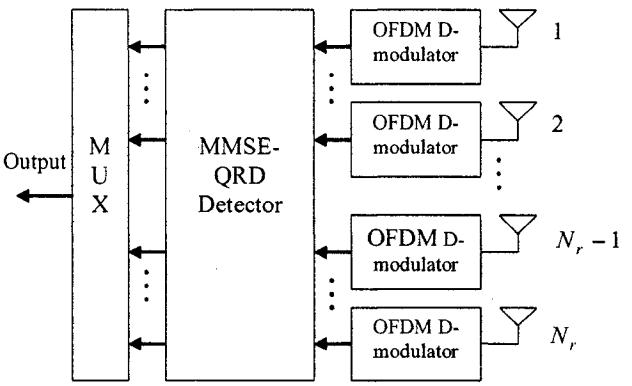

Figure 4.3: MLSTBC-OFDM decoder structure.

4.4 Space-Frequency-Time Codes for MIMO Systems

STC offers diversity gain by coding over the space and time dimensions. Transmitting data over MIMO-OFDM systems is feasible by utilizing STC to each sub-carrier. This does not provide the maximum achievable diversity gain. In reality, the frequency diversity and the correlation among diverse sub-carriers are mistreated in such a system [31]. To attain the maximum achievable diversity gain, one could code over the three dimensions of space, time, and frequency as shown in Figure 4.4 [31]. Thus, by transmitting the codeword over different sub-carriers we can provide additional frequency diversity. This may be achieved by employing error correcting codes and interleaving [32]. Interleaving ensures that the coding is over space, time, and frequency. In order to extract frequency diversity from the multipath

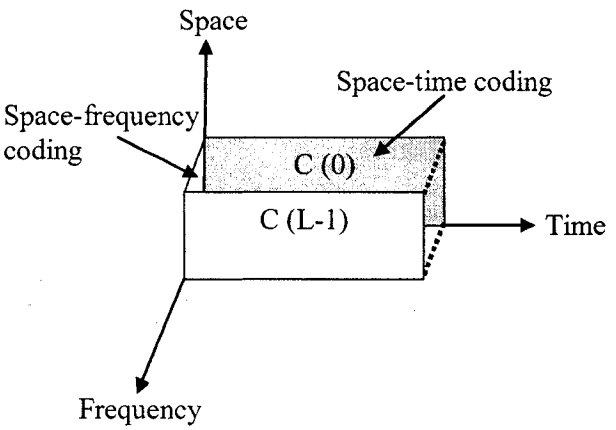

Figure 4.4: Space, time, frequency dimension.

channel, we must use an outer error correcting code.

SFT coding for OFDM applies spatial coding across multiple antennas, frequency coding across OFDM subcarriers and temporal coding across consecutive OFDM symbols. The initial SFT coding analysis was completed by [29] where they modified Tarokh's STC [5] to work with OFDM technology. Nonetheless, these codes were initially designed for quasi-static fading channels. While they are used in conjunction with OFDM to combat a frequency selective channel, they do not take advantage of the frequency dimension. Consequently, they are not optimized for frequency selective channels and do not take advantage from the available frequency diversity. In [42], [43], and [44] it was established that the maximum achievable diversity for a MIMO-OFDM system is pN_tN_r, where p is the number of paths in the frequency selective channel. We wish to modify the existing MLSTBC-OFDM scheme

to extract from the multipath channel the frequency diversity. In order to accomplish this, we must use SFT technology. We propose a multilayered SFT OFDM scheme that employs the Alamouti algorithm at each subgroup and call it MLSFTBC-OFDM.

4.4.1 System Model of MLSFTBC-OFDM

The system model of the MLSFTBC-OFDM scheme is similar to that of the MLSTBC-OFDM scheme described in the previous section, except that we concatenate an error correcting code. We choose to concatenate a convolutional code (CC) to the MLSTBC-OFDM system and transform it into the MLSFTBC-OFDM scheme. This will enable the maximal achievable diversity order not only to increase with the number of transmit and receive antennas, but also with the number of channel paths. Furthermore, the maximum diversity attainable is dependent on the Hamming distance $d^H_{\min}$ of the employed CC. We must also place an interleaver after the CC encoder. Interleaving in a MIMO system will ensure that the transmitted signal is adequately spread over time and/or frequency.

We can represent the half rate codeword at the output of the CC encoder for the case of the Alamouti scheme being used at the kth subgroup to be

$$C_k = c_{k,1}(0)c_{k,2}(0)c_{k,1}(1)c_{k,2}(1)\ldots c_{k,1}(N_{FFT}-1)c_{k,2}(N_{FFT}-1).$$

Thus for the Alamouti scheme ($n = 2$), for a given symbol period, and for each subgroup, the OFDM block transmitted from the first antenna is

$$C_{k,1} = c_{k,1}(0)c_{k,1}(1)\ldots c_{k,1}(N_{FFT}-1),$$

and the OFDM block sent to the second antenna is

$$C_{k,2} = c_{k,2}(0)c_{k,2}(1)\ldots c_{k,2}(N_{FFT}-1).$$

The codeword then passes through a block interleaver with depth equal to one OFDM symbol. The interleaving depth is equal to one OFDM symbol since the channel is assumed to be quasi-static; thus the channel is assumed to be the same for the duration of one OFDM symbol. The codeword then passes to the STBC encoder and finally to the OFDM modulators as shown in Figure 4.5.

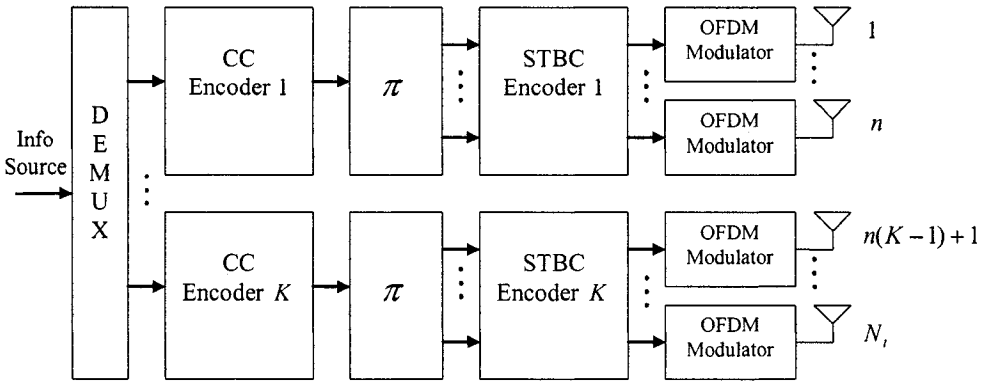

Figure 4.5: MLSFTBC-OFDM transmitter structure.

4.4.2 Decoder for MLSFTBC-OFDM

The decoding process for the proposed MLSFTBC-OFDM system is identical to that of the MLSTBC-OFDM decoding process except that a Viterbi algorithm must be applied after the decoding process of the MLSFTBC-OFDM decoder. Also at the output of the MMSE-QRD detector, soft decisions will be used to enter the Viterbi decoder rather than hard decisions. Figure 4.6 demonstrates the decoding process of the MLSFTBC-OFDM system.

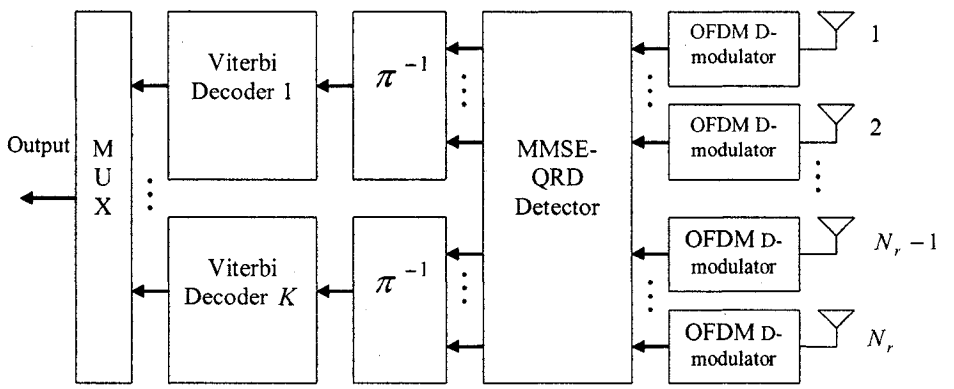

Figure 4.6: MLSFTBC-OFDM decoder structure.

Now we would like to apply the MMSE-QRD detector to the MLSFTBC-OFDM system.

To do this we must first use the equivalent channel matrix $\mathbf{H}_{eq}$ at time t. For the Alamouti case where two transmit antennas are applied at each subgroup, $\mathbf{H}_{eq}$ is given as

$$\mathbf{H}_{eq} = \begin{bmatrix} \mathbf{h}_{1,1} & \mathbf{h}_{1,2} & \cdots & \mathbf{h}_{1,N_t} \\ \mathbf{h}_{2,1} & \mathbf{h}_{2,2} & \cdots & \mathbf{h}_{2,N_t} \\ \vdots & \ddots & \cdots & \vdots \\ \mathbf{h}_{N_r,1} & \mathbf{h}_{N_r,2} & \cdots & \mathbf{h}_{N_r,N_t} \\ (\mathbf{h}_{1,2})^* & -(\mathbf{h}_{1,1})^* & \cdots & -(\mathbf{h}_{1,N_t-1})^* \\ (\mathbf{h}_{2,2})^* & -(\mathbf{h}_{2,1})^* & \cdots & -(\mathbf{h}_{2,N_t-1})^* \\ \vdots & \cdots & \ddots & \vdots \\ (\mathbf{h}_{N_r,2})^* & -(\mathbf{h}_{N_r,1})^* & \cdots & -(\mathbf{h}_{N_r,N_t-1})^* \end{bmatrix},$$

where $(\cdot)^*$ is the conjugate of the element. Thus the received signal is now

$$\mathbf{Z} = \mathbf{H}_{eq}\mathbf{X} + \mathbf{N}.$$

We can not directly apply the MMSE-QRD detector on the equivalent channel matrix. We must extend the equivalent channel matrix as such

$$\bar{\mathbf{H}} = \begin{bmatrix} \mathbf{H}_{eq} \\ \delta_n \mathbf{I}_{N_t} \end{bmatrix},$$

where $\mathbf{I}_{N_t}$ is a $N_t \times N_t$ identity matrix and δ_n is the standard deviation of the noise term. We continue by extending the received matrix $\mathbf{Z}$ as follows

$$\bar{\mathbf{Z}} = \begin{bmatrix} \mathbf{Z} \\ \mathbf{0}_{N_t,L} \end{bmatrix},$$

where $\mathbf{0}_{N_t,L}$ is a $N_t \times L$ zero matrix. We then take the QRD of the extended channel matrix $\bar{\mathbf{H}} = \mathbf{QR}$, where the $(N_r n + N_t) \times N_t$ matrix $\mathbf{Q}$ has orthonormal columns and the $N_t \times N_t$ matrix $\mathbf{R}$ is upper triangular. Following this, we may apply the detection algorithm for MLSTBC to detect each subcarrier of the OFDM symbols.

4.4.3 Performance Analysis of MLSFTBC-OFDM Systems

To analyze the performance of the MLSFTBC-OFDM system, we must first assume the maximum likelihood decoding of the scheme. The overall performance of the MLSFTBC-OFDM scheme is limited by the performance of the first group detected. Thus in our analysis we will refer to the first group detected performance results. Assuming that ideal channel knowledge is available at the receiver for a specified realization of channel $\mathbf{H}$, the conditional pairwise error probability of transmitting $\mathbf{X}$ and concluding in favour of another codeword $\hat{\mathbf{X}}$ at the decoder conditioned on $\mathbf{H}$ is given by [19]

$$P\left(\mathbf{X}, \hat{\mathbf{X}} \mid \mathbf{H}\right) \leq \exp\left(-\delta_H^2(\mathbf{X}, \hat{\mathbf{X}}) \frac{E_s}{4N_0}\right),$$

where δ_H^2 is a modified Euclidean distance between the two space-time codeword matrices $\mathbf{X}$ and $\hat{\mathbf{X}}$, given by [19]

$$\begin{aligned}
\delta_H^2(\mathbf{X}, \hat{\mathbf{X}}) &= \sum_{j=1}^{N_r} \sum_{k=1}^{N_{FFT}} \left| \sum_{i=1}^{N_t} H_{j,i}^k (x_k^i - \hat{x}_k^i) \right|^2 \\
&= \sum_{j=1}^{N_r} \sum_{k=1}^{N_{FFT}} \left| \sum_{i=1}^{N_t} (\mathbf{h}_{j,i}^t)^H \cdot \mathbf{w}_k \cdot (x_k^i - \hat{x}_k^i) \right|^2 \\
&= \sum_{j=1}^{N_r} \sum_{k=1}^{N_{FFT}} \left| \mathbf{h}_j^t \mathbf{W}_k \mathbf{e}_k \right|^2,
\end{aligned}$$

where

$$\begin{aligned}
\mathbf{h}_j^t &= \left[\left(\mathbf{h}_{j,1}^t\right)^H, \left(\mathbf{h}_{j,2}^t\right)^H, \ldots, \left(\mathbf{h}_{j,N_t}^t\right)^H \right], \\
\mathbf{W}_k &= \begin{bmatrix} w_k & 0 & \cdots & 0 \\ 0 & w_k & \cdots & 0 \\ \vdots & \vdots & \ddots & \vdots \\ 0 & 0 & \cdots & w_k \end{bmatrix},
\end{aligned}$$

and

$$\mathbf{e}_k = \begin{bmatrix} x_k^1 - \hat{x}_k^1 \\ x_k^2 - \hat{x}_k^2 \\ \vdots \\ x_k^{N_t} - \hat{x}_k^{N_t} \end{bmatrix}.$$

In [19] it was established that the rank of $\delta_H^2(\mathbf{X}, \hat{\mathbf{X}})$ is given by

$$r_h \leq \min(d_{\min}^H, pN_t).$$

Provided that the Hamming distance $d_{\min}^H$ of the CC applied must satisfies this condition [19]

$$d_{\min}^H \geq pN_t,$$

from this we can establish that the maximum achievable diversity gain for MLSFTBC-OFDM using the maximum likelihood detector is pN_tN_r. This however is achieved with dependency on the Hamming distance of the employed CC, which plays a significant role in attaining the effective diversity order from the multipath channel.

The maximum diversity order pN_tN_r is achieved with the maximum likelihood detector. Since we are dealing with the MLSFTBC-OFDM scheme, the maximum transmit diversity will be pn, where n is the number of transmit antennas from each subgroup (we assume that all sub-groups have the same number of transmit antennas). However, the maximum likelihood detector is a very complex detector. Since in our system we apply the MMSE-QRD detector as explained in the previous section, we will not obtain N_r as the receive diversity order. As mentioned earlier in the chapter, the receive diversity achieved by the MMSE-QRD detector for the first detected subgroup of the MLSTBC-OFDM system will be $(N_r - K + 1)$. Thus the maximum diversity order achievable by the MLSFTBC-OFDM system applying the MMSE-QRD detector is

$$d = pn \times (N_r - K + 1).$$

It was established in [45] that there is a loss in diversity advantage that exist with OFDM schemes. Thus the maximum diversity order is not in reality $pn \times (N_r - K + 1)$. The maximum achievable transmit diversity is in fact

$$p(n-1) + 1.$$

The proof of this diversity results, is in direct relation to the Singleton bound [45], [46].

Thus the maximum overall transmit diversity of the MLSFTBC-OFDM system with the MMSE-QRD detector for the kth detected layer is

$$d_{MLSFTBC-OFDM} = (p(n-1) + 1) \times (N_r - k + 1).$$

We may re-write the condition on achieving the maximum diversity on the Hamming distance of the CC as

$$d^H_{\min} \geq pn.$$

For example for a system with $n = 2$, $p = 2$, and Hamming distance $d^H_{\min} = 5$. The maximum diversity order will be achieved, however for path number greater than 2, this condition will not be satisfied, and thus the maximum achievable diversity gain will not be achieved. Hence in this case a CC with a greater Hamming distance will be used.

This transmit diversity loss can be eased at the price of additional amplification in the peak-to-average power ratio and complexity, by means of multidimensional rotated constellations [45].

4.5 Simulation Results

The MLSFTBC-OFDM system was simulated using BPSK modulation. Each layer is encoded by a separate rate 1/2 convolutional code. The output of the two convolutional encoders are interleaved as described above, and the output of the interleaver is applied to two independent STBC encoders, each employing the Alamouti scheme. At the receiver end the MMSE-QRD detector is applied. Hard decision Viterbi decoding is considered. We have assumed a slow frequency selective channel that remains static for each OFDM symbol. We use a 64-subcarrier OFDM system. We assume perfect channel knowledge at the receiver.

In Figure 4.7 we demonstrates the BER performance of a MLSFTBC-OFDM $(4, 2, 2)$ system with different number of multipaths $p = 1, 2, 3$. The CC applied to this system is a rate 1/2 convolutional code with generator polynomials $(171, 133)_{oct}$, thus $d^H_{\min} = 10$. The performance results are for the overall performance (all layers) with error propagation at each detection stage. Also included in the figure are the theoretical results. These theoretical results follow the pairwirse error probability of a MIMO system with CC coding as

$$P_b \leq \sum_{d=d^H_{\min}}^{\infty} \beta_d P_2(d), \tag{4.5}$$

where β_d denotes the number of paths of distance d from the all-zero path for the first time [23] and

$$P_2(d) \approx \binom{2d_{sys}}{d_{sys}} (4R_c d\rho)^{-d_{sys}},$$

where d_{sys} is the diversity of the system, R_c is the rate of the convolutional code, and

$\rho = \frac{E_b}{N_t N_0}$. From the figure, it is obvious that including OFDM in the MLSTBC system has successfully transformed the frequency selective channel into N_{FFT} parallel flat fading channels. The theoretical results from (4.5) in the figure were plotted for $d_{sys} = 2, 3, 4$.

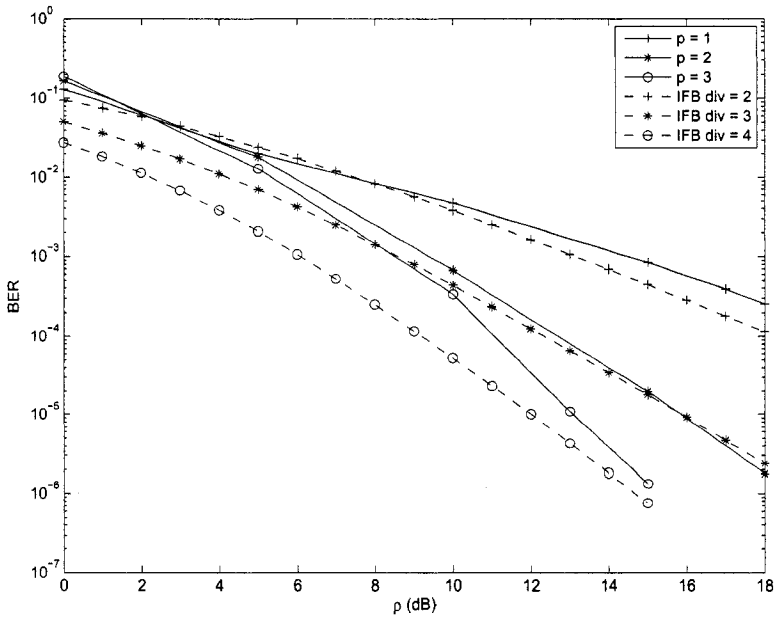

Figure 4.7: BER performance of $(4, 2, 2)$ MLSTBC-OFDM system on various multipath fading channels.

In Figure 4.8 we plot the BER performance of a MLSFTBC-OFDM $(4, 2, 2)$ system with different number of multipaths $p = 1, 2, 3$. The CC applied to this system is a rate $1/2$ convolutional code with generator polynomials $(7, 5)_{oct}$, thus $d^H_{\min} = 5$. From this figure, it is shown that the minimum Hamming distance has an impact on the performance results of the MLSFTBC-OFDM system. We observe that as the paths in the frequency selective channel increases, the system's ability to retrieve the frequency diversity is diminished. In fact with the theoretical results plotted in the same figure with $d_{sys} = 2, 3$, we observe that the diversity will not increase more than 3.

In Figure 4.9 we plot the BER performance of a MLSFTBC-OFDM $(4, 2, 3)$ system with different number of multipaths $p = 1, 2, 3$. The CC applied to this system is a rate $1/2$ convolutional code with generator polynomials $(171, 133)_{oct}$, with $d^H_{\min} = 10$. We can conclude that the system has adequately combated the frequency selective channel, as well as extracted frequency diversity. We observe that the system with $p = 2$, achieves a diversity gain of 3×2, while the system with $p = 3$ has a diversity gain of 4×2.

In Figure 4.10 we demonstrate the BER performance of a MLSFTBC-OFDM $(4, 2, 4)$

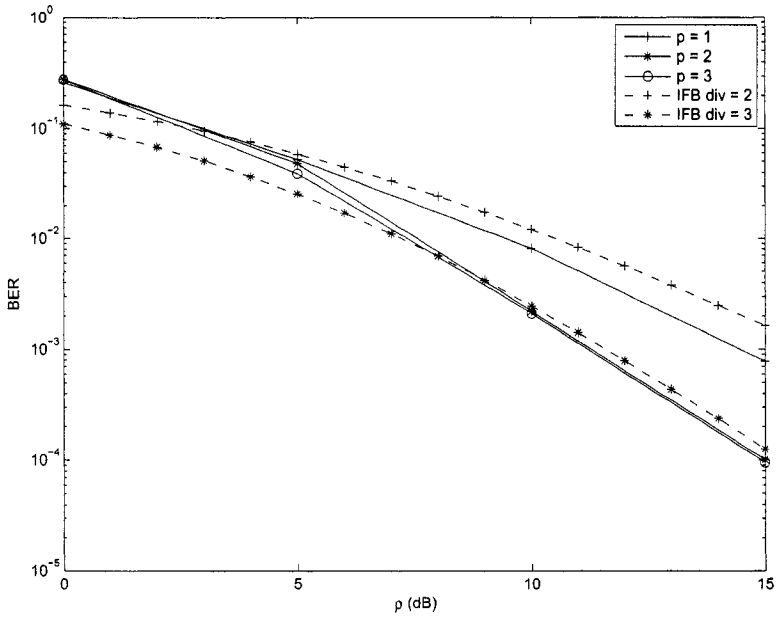

Figure 4.8: BER performance of $(4, 2, 2)$ MLSTBC-OFDM system on various multipath fading channels with $d^H_{\min} = 5$.

system with different number of multipaths $p = 1, 2$. The CC applied to this system is a rate $1/2$ convolutional code with generator polynomials $(171, 133)_{oct}$, with $d^H_{\min} = 10$. The system with $p = 1$ experiences a diversity gain of 2×3, while the system with $p = 2$, has a diversity gain of 3×3.

4.6 Chapter Summary

In this chapter we have extended the MLSTBC system to function in a frequency selective channel. This was accomplished by adding OFDM technology to the system in order to combat ISI caused by the multipath fading channel. We showed that by adding a convolutional code and simple interleaver that frequency diversity can be extracted to increase the performance of the system.

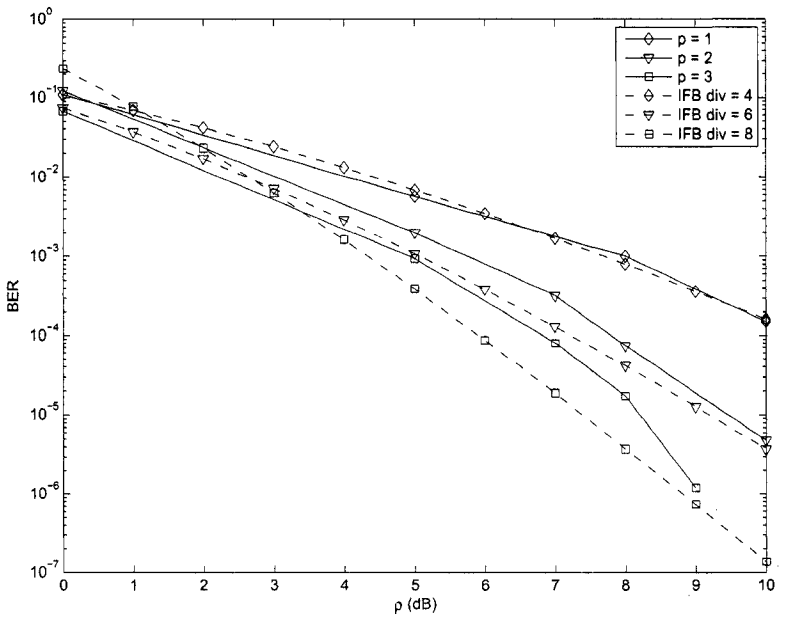

Figure 4.9: BER performance of $(4, 2, 3)$ MLSTBC-OFDM system on various multipath fading channels.

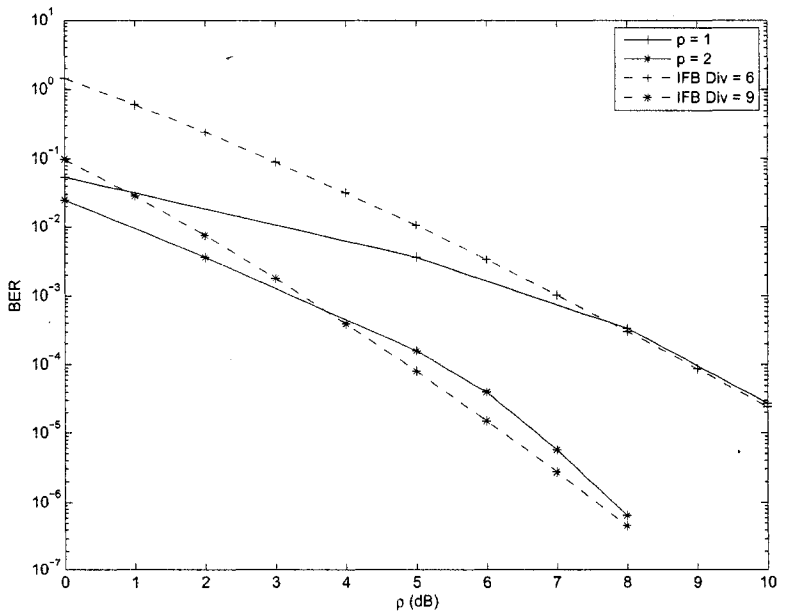

Figure 4.10: BER performance of $(4, 2, 4)$ MLSTBC-OFDM system on various multipath fading channels.

Chapter 5

A New Transceiver Architecture for Multilayered Space-Time Coded MIMO Systems

5.1 Introduction

In MIMO systems with N_t transmit and N_r receive antennas, it has been shown that the capacity increases by $\min(N_t, N_r)$ bits per channel use for every 3.0 dB increase in the SNR [1]. Additionally, the maximum spatial diversity that can be achieved over quasi-static fading channels is $N_t N_r$. As mentioned in previous chapters, the coding schemes that can achieve this diversity include STTCs and STBCs, rendering such codes very effective in combatting the adverse effects of fading. However, these coding schemes achieve a spatial rate of unity or less without offering flexibility in trading diversity for rate. Providing such a trade-off is essential to accommodate a wide range of wireless applications, especially those applications that have high data rate requirements. The notion of LST coding [2], first introduced by Foschini in 1996, has emerged since then as a powerful architecture suitable for applications with high data rates. As described in pervious chapter, several LST coding architectures exist, including the H-BLAST, the V-BLAST, and the D-BLAST architectures. A common feature of these architectures is that N_t independent data substreams are transmitted simultaneously from the available N_t transmit antennas. Consequently, these LST architectures achieve a spatial rate of $R_c b N_t$ where R_c denotes the rate of the channel code employed and 2^b denotes the signal constellation size.

Other LST schemes exist, including the MLSTC scheme proposed in [20], and the threaded space-time coding (TSTC) scheme proposed in [47]. As explained earlier, the

MLSTC scheme merges coding concepts at the transmitter and signal array processing at the receiver in an effort to trade rate for diversity. In particular, the MLSTC scheme divides the transmit antennas into subgroups and each subgroup has its corresponding STC. One disadvantage of the MLSTC scheme is that the overall performance is dominated by the first detected layer, which normally has a low diversity order. The TSTC architecture, on the other hand, is designed to take full advantage of the diversity available in the MIMO channel. This is achieved by spreading the transmitted codeword in a way such that it spans the entire spatial and time dimensions. The TSTC architecture is superior to the MLSTC architecture at the same transmission rate. The performance gain of TSTC is credited to its iterative MMSE receiver, which has high computational complexity.

In this chapter, we present a new transceiver architecture for MIMO systems that borrows ideas from the MLSTC and TSTC schemes in an effort to achieve an enhanced trade-off between the spatial rate and diversity. Therefore, we refer to the proposed scheme as threaded MLSTC (TMLSTC). Specifically, the proposed scheme has a structure similar to that of the MLSTC scheme except that it employs a spatial interleaver just before the MLSTC encoder. The reason for using the spatial interleaver is to take full advantage of the spatial and time diversity available in the channel, whereas the use of the MLSTC encoder is to maintain a reasonable decoding complexity. We also propose a low complexity MMSE-based decoder for this coding scheme which incorporates the QR decomposition (QRD). The advantages of the proposed scheme over existing ones include: 1) considerable improvement in performance; 2) enhanced trade-off between rate and diversity; and 3) all layers achieve the same performance and rate and hence the same capacity, which is attractive for multiuser environments.

5.2 Proposed Transceiver Architecture TMLSTC

5.2.1 Proposed Architecture

We consider a MIMO system with N_t transmit and N_r receive antennas. The proposed transmitter architecture is shown in Figure 5.1. In the proposed scheme, as shown in the figure, the input information sequence is initially demultiplexed into N_t substreams. Each substream is then encoded separately by a channel encoder, modulated and then passed through a spatial interleaver (SI). The SI may be represented by a cyclic shift interleaver as

$$x_{i',t} = x_{i,t}, \text{ with } i' = [(i + t - 2) \bmod N_t] + 1, \tag{5.1}$$

where $x_{i',t}$ represents the entries of the threaded transmission matrix, i indicates the antenna number, and t represents the time interval [19].

Assume that there are K layers, that is, the N_t transmit antennas are divided equally into K groups where each group consists of $n = N_t/K$ antennas. As such, the N_t coded substreams are multiplexed into K substreams to match the number of transmit antenna groups. Each group of antennas employs a STBC. (This is not limited to STBCs, where other STCs can be employed as well.) The K STBCs are independent. The number of receive antennas must satisfy the condition $N_r \geq K$. The TMLSTC system can be presented as (N_t, n, N_r). Since we are using STBC encoders we will refer to our architecture as TMLSTBC from now on.

Let

$$\mathbf{X} = \begin{bmatrix} x_{1,1} & \cdots & x_{1,L} \\ \vdots & \ddots & \vdots \\ x_{N_t,1} & \cdots & x_{N_t,L} \end{bmatrix} \tag{5.2}$$

denote the $N_t \times L$ transmit signal matrix where L is the frame length. Each row represents the symbols transmitted by each transmit antenna.

In a TMLSTBC scheme, the overall transmit signal matrix can be described by stacking all the signal matrices resulting from each STBC encoder $\mathbf{G}_i(x)$, for $i = 1, 2, \ldots, K$ as

$$\mathbf{G}(x) = \begin{bmatrix} \mathbf{G}_1(x) & \mathbf{G}_2(x) & \cdots & \mathbf{G}_K(x) \end{bmatrix}^T. \tag{5.3}$$

For example, for a $(4, 2, 4)$ TMLSTBC system, the number of antenna groups is two and each group employs the Alamouti scheme. When $L = 1$, $\mathbf{G}(x)$ can be written as

$$\mathbf{G}(x) = \begin{bmatrix} x_{1,1} & -x_{2,1}^* & x_{3,1} & -x_{4,1}^* \\ x_{2,1} & x_{1,1}^* & x_{4,1} & x_{3,1}^* \end{bmatrix}^T. \tag{5.4}$$

Assuming quasi-static flat fading, the received signal can now be expressed as

$$\mathbf{Y} = \mathbf{H}\mathbf{G}(x) + \mathbf{N}, \tag{5.5}$$

where $\mathbf{H}$ is the fading coefficient matrix of size $N_r \times N_t$ with elements $h_{i,j}$ representing the fading gains between the jth transmit antenna and the ith receive antenna. These fading coefficients are assumed to be independent and $\mathcal{CN}(0, 1)$ distributed. The matrix $\mathbf{N}$ is composed of $\mathcal{CN}(0, N_0)$ distributed noise samples with a size of $N_r \times nL$. Note that the

first n columns of $\mathbf{H}$ correspond to the first layer, the second n columns correspond to the second layer, and so on. As such, we can can express $\mathbf{H}$ as $\begin{bmatrix} \mathbf{H}_1 & \mathbf{H}_2 & \cdots & \mathbf{H}_K \end{bmatrix}$.

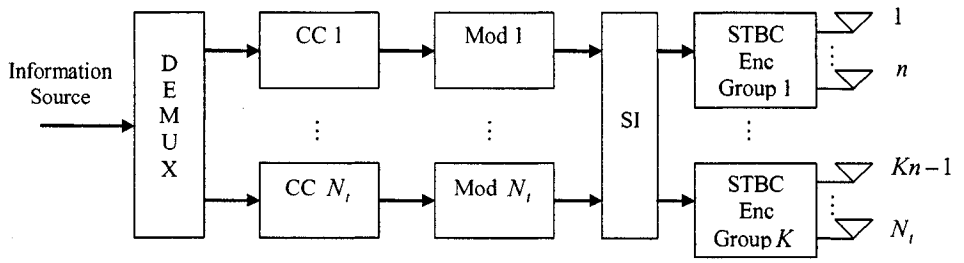

Figure 5.1: Proposed transmitter structure.

5.2.2 Proposed MMSE-QRD Decoder

The decoder used in [20] for the MLSTC architecture is the group interference cancellation (GIC) decoder. The TSTC architecture uses an iterative MMSE decoder. Our proposed TMLSTC architecture uses a decoder that is less complex than these decoders while maintaining their advantages. It was shown in [24] that one could incorporate the MMSE criterion into the QRD (MMSE-QRD), which in turn can be applied to the MLSTC architecture. It was established that the MMSE-QRD receiver delivers improved performance with lower computational complexity. Additionally, the MMSE-QRD decoder also allows for the number of receive antennas to be less than that of the transmit antennas. We can apply the MMSE-QRD receiver to the TMLSTBC architecture. To this end, we re-write the received signal in (5.5) as

$$\mathbf{Z} = \mathbf{H}_{eq}\mathbf{X}' + \mathbf{N}_{eq},$$

where $\mathbf{H}_{eq}$ is the equivalent channel matrix of dimension $(N_r n) \times N_t$, $\mathbf{N}_{eq}$ is the equivalent noise matrix, and the SI transmitted signal is now represented in the $(N_t \times L)$ matrix $\mathbf{X}'$.

For example if we are employing the Alamouti scheme for a $(4, 2, 4)$ MIMO system with $L = 4$, we can represent the equivalent channel matrix $\mathbf{H}_{eq}$ as

$$\mathbf{H}_{eq} = \begin{bmatrix} h_{1,1} & \cdots & h_{4,1} & h_{1,2}^* & \cdots & h_{4,2}^* \\ \vdots & \ddots & \vdots & \vdots & \ddots & \vdots \\ h_{1,4} & \cdots & h_{4,4} & -h_{1,3}^* & \cdots & -h_{4,3}^* \end{bmatrix}^T,$$

and the SI transmitted matrix following (5.1) as

$$\mathbf{X}' = \begin{bmatrix} x_{1,1} & x_{2,2} & x_{3,3} & x_{4,4} \\ \vdots & \vdots & \vdots & \vdots \\ x_{4,1} & x_{1,2} & x_{2,3} & x_{1,4} \end{bmatrix}.$$

The MMSE filter matrix is given as

$$\mathbf{G}_{MMSE} = (\mathbf{H}^H\mathbf{H} + \delta_n^2\mathbf{I}_{N_t})^{-1}\mathbf{H}^H,$$

where $\delta_n^2 = N_0$ is the noise variance and $\mathbf{I}_{N_t}$ is a $N_t \times N_t$ identity matrix. In [24], the authors demonstrate that with the definition of an extended channel matrix

$$\bar{\mathbf{H}} = \begin{bmatrix} \mathbf{H} & \delta_n\mathbf{I}_{N_t} \end{bmatrix}^T,$$

with size $(N_r + N_t) \times N_t$, and an extended receive matrix

$$\mathbf{Y}' = \begin{bmatrix} \mathbf{Y} & \mathbf{0}_{N_t} \end{bmatrix}^T,$$

of size $(N_r + N_t) \times nL$, where $\mathbf{0}_{N_t}$ is a $N_t \times N_t$ zero matrix , the MMSE filter matrix may be rewritten as

$$\mathbf{G}_{MMSE} = (\bar{\mathbf{H}}^H\bar{\mathbf{H}})^{-1}\bar{\mathbf{H}}^H.$$

To enable the MMSE-QRD decoder to work for a multilayered system, we must use the equivalent channel matrix $\mathbf{H}_{eq}$ to provide a $(N_r n + N_t) \times N_t$ extended channel matrix

$$\bar{\mathbf{H}} = \begin{bmatrix} \mathbf{H}_{eq} & \delta_n\mathbf{I}_{N_t} \end{bmatrix}^T,$$

and a $(N_r n + N_t) \times L$ extended receive matrix

$$\mathbf{Z}' = \begin{bmatrix} \mathbf{Z} & \mathbf{0}_{N_t} \end{bmatrix}^T.$$

We then take the QRD of the extended channel matrix $\bar{\mathbf{H}} = \mathbf{QR}$, where the $(N_r n + N_t) \times N_t$ matrix $\mathbf{Q}$ has orthonormal columns and the $N_t \times N_t$ matrix $\mathbf{R}$ is upper triangular. We may

further expand the QR decomposition into

$$\bar{\mathbf{H}} = \mathbf{QR} = \begin{bmatrix} \mathbf{Q}_1\mathbf{R} & \mathbf{Q}_2\mathbf{R} \end{bmatrix}^T,$$

where the matrix $\mathbf{Q}$ was divided into the $N_r n \times N_t$ matrix $\mathbf{Q}_1$, and the $N_t \times N_t$ matrix $\mathbf{Q}_2$. From knowing that

$$\mathbf{Q}^H\bar{\mathbf{H}} = \mathbf{Q}_1^H\bar{\mathbf{H}} + \delta_n\mathbf{Q}_2^H = \mathbf{R}.$$

We should pre-multiply $\mathbf{Q}^H$ with the extended receive matrix $\mathbf{Z}'$ to obtain the decision statistics of the transmitted signals as

$$\tilde{\mathbf{Z}} = \mathbf{Q}^H\mathbf{Z}' = \mathbf{Q}_1^H\mathbf{Z} = \mathbf{RX}' - \mathbf{N}_0\mathbf{R}^{-H}\mathbf{X}' + \mathbf{Q}_1^H\mathbf{N}_{eq}, \tag{5.6}$$

where $\tilde{\mathbf{Z}}$ is of size $(N_t \times L)$. By writing $\tilde{\mathbf{Z}}$ in an expanded form, we can write the (i,t)th element as

$$\tilde{z}_{i,t} = r_{i,i}x'_{i,t} + \sum_{k=i+1}^{N_t} r_{i,k}x'_{k,t} + \tilde{n}_{i,t},$$

where $\tilde{n}_{i,t}$ is the corresponding noise term. Note that the (i,t)th element of $\tilde{\mathbf{Z}}$ corresponds to the (i,t)th element of $\mathbf{X}'$. Now to obtain the desired symbol, its interference contribution is calculated and subtracted from the received signal as

$$\tilde{z}_{i,t} = \tilde{z}_{i,t} - \sum_{k=i+1}^{N_t} r_{i,k}\hat{x}_{k,t}.$$

The first substream detected in the detection process is the N_tth substream due to the upper triangular properties of the matrix $\mathbf{R}$. The $(N_t - 1)$th substream is subsequently detected. This process continues until the first substream is detected. Afterwards, the N_t detected substreams are de-interleaved, de-modulated, and each substream is sent to its individual corresponding Viterbi decoder. Thereafter, the N_t decoded substreams are re-grouped into K groups by taking n consecutive substreams to make a group. Figure 5.2, and 5.3 depict the block diagrams of the receiver and the MMSE-QRD detector structures respectively.

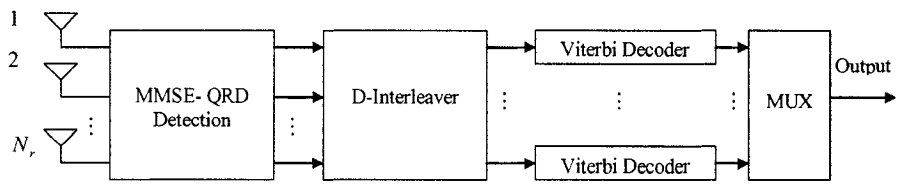

Figure 5.2: Proposed receiver structure.

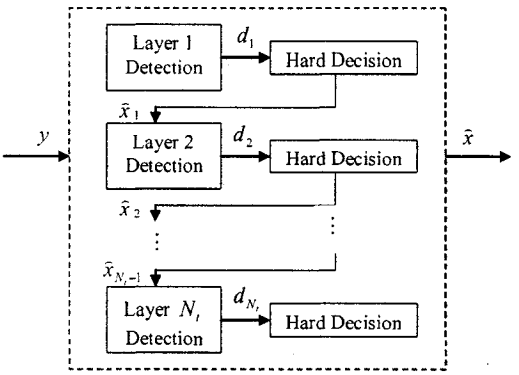

Figure 5.3: MMSE-QRD detector structure.

5.3 Performance Analysis of TMLSTBC

5.3.1 Diversity of the Proposed Scheme

For the MLSTBC scheme using the GIC detector, the kth detected group achieves a diversity gain of

$$n_k \times (n_1 + n_2 + \cdots + n_k + N_r - N_t),$$

where n_k is the number of antennas corresponding to the kth subgroup [20]. The overall system performance is limited by the performance of the first group. Hence, the overall performance of the MLSTBC architecture at high SNR values can approximated as [23]

$$P_b \approx \binom{2n(n+N_r-N_t)-1}{n(n+N_r-N_t)} (4\rho)^{-n(n+N_r-N_t)}, \tag{5.7}$$

where $\rho = \frac{E_b}{N_t N_0}$.

As shown in the previous chapter, the diversity of the MLSTBC scheme is increased with

the MMSE-QRD detector. The diversity for the overall system was shown to be

$$d_{MLSTBC-MMSE_{QRD}} = n \times (N_r - K + 1),$$

which is an increase to the diversity order of the MLSTBC scheme with the GIC detector.

For the TMLSTBC structure, the SI causes spatial spreading from all layers across all antennas. Accordingly, the symbols belonging to a codeword are detected at various steps of the detection process. Thus a diversity of N_r can be gained, making all groups benefit from the same diversity gain. We can establish that the achievable diversity order is nN_r. At high signal to noise ratio, ρ, the pairwise error probability for the proposed scheme is given by

$$P_2(d) \approx \binom{2nN_r - 1}{nN_r} (4R_c d\rho)^{-nN_r}, \tag{5.8}$$

where $d = d^H_{\min}$ for soft decision Viterbi decoding and $d = d^H_{\min}/2$ for hard decision Viterbi decoding. $d^H_{\min}$ and R_c are the minimum Hamming distance and rate of the convolutional code, respectively. The average bit error rate can be found as

$$P_b \leq \sum_{d=d^H_{\min}}^{\infty} \beta_d P_2(d), \tag{5.9}$$

where β_d denotes the number of paths of distance d from the all-zero path for the first time [23]. Comparing (5.7) and (5.8), it is evident that the new scheme achieves better performance when $n \leq N_r$. For a square MIMO system, this will always hold.

5.3.2 Diversity-Multiplexing Gain Trade-off

It was established is [48] that the optimal diversity-multiplexing gain trade-off curve can assist to compare the performance of various architectures. In this section, we derive the diversity-multiplexing gain trade-off curves for the TMLSTBC and MLSTBC architectures. We know that the capacity of a MIMO channel is

$$C = \log\det\left(\mathbf{I}_{N_r} + \frac{\rho}{N_t}\mathbf{H}\mathbf{H}^H\right)$$

where ρ is the average SNR. Suppose we want to communicate at a goal rate of R bits per channel use. We can realize dependable communication provided that $C > R$. When the MIMO channel does not satisfy this condition, the system is in outage.

At high ρ values, it has been shown in [48] that a diversity gain $d(r)$ is achieved at

multiplexing gain r if $R = r \log \rho$, and

$$P_{out}(R) \approx \rho^{-d(r)},$$

or more precisely

$$\lim_{\rho \to \infty} \frac{\log P_{out}(r \log \rho)}{\log \rho} = -d(r).$$

The curve found from $d(r)$ represents the diversity-multiplexing gain trade-off. From [48] and [9], it was shown that the optimal trade-off curve for a MIMO system is

$$d(r) = (N_t - r)(N_r - r).$$

Let R_i for $i = 1, 2, \ldots, K$ denote the rate corresponding to the ith layer. As such, we can write $R_i = (r/K) \log \rho$ (bits/symbol) for the MLSTBC and TMLSTC schemes. At high ρ, the outage probability for the ith layer is upper bounded by

$$P_{out}(R_i) = P\left\{1 + \frac{\rho}{N_t} \|\mathbf{H}_i\|^2 < r \log \rho\right\},$$

where $\mathbf{H}_i$ is the channel matrix corresponding to the ith layer. $\|\mathbf{H}_i\|^2$ is a chi-squared distributed random variable. Since the overall performance for both the MLSTBC and TMLSTBC schemes is limited by the performance of the first detected layer, we will focus on the first layer. Hence for the MLSTBC scheme, $\|\mathbf{H}_1\|^2$ is a chi-squared distributed random variable with $2n(n + N_r - N_t)$ degrees of freedom. Thus the overall outage probability will be

$$\begin{aligned} P_{out}(R_i) &= P\left\{1 + \frac{\|\mathbf{H}_1\|^2 \rho}{N_t} < \rho^r\right\} \\ &= P\left\{\|\mathbf{H}_1\|^2 < \rho^{-(1-r)}\right\} \\ &= \rho^{-n(n+N_r-N_t)(1-r/K)}. \end{aligned}$$

Thus, the overall trade-off curve of the MLSTBC scheme is

$$d(r) = n(N_r - N_t + n)(1 - r/K).$$

For the TMLSTBC scheme, $\|\mathbf{H}_1\|^2$ is a chi-squared distributed random variable with $2nN_r$

degrees of freedom. The outage probability then becomes

$$\begin{aligned} P_{out}(R_i) &= P\left\{1+\frac{\rho}{N_t}\left\|\mathbf{H}_i\right\|^2 < \rho^r\right\} \\ &= P\left\{\left\|\mathbf{H}_i\right\|^2 < \rho^{-(1-r)}\right\} \\ &= \rho^{-nN_r(1-r/K)}, \end{aligned}$$

thus

$$d(r) = nN_r(1-r/K),$$

is the diversity-multiplexing gain trade-off curve achieved by TMLSTBC.

Figure 5.4 demonstrates the optimal trade-off curve for a $(4,4)$ MIMO system and compares it to the trade-off curves of a $(4,2,4)$ MLSTBC, and the proposed TMLSTBC systems. From the figure, it is evident that the TMLSTBC scheme achieves a better trade-off between the rate and the diversity than the MLSTBC scheme.

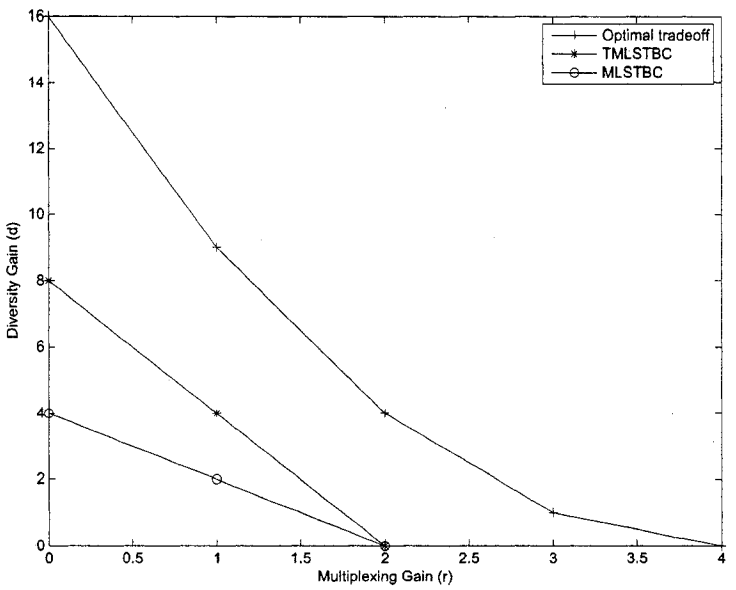

Figure 5.4: Tradeoff curve for $(4,2,4)$ system.

In Table 5.1, we present the rate and diversity trade-off of various schemes. We compare their maximum attainable diversity and spatial multiplexing gain.

From this table we can observe that our proposed scheme attains the highest diversity at the cost of some spatial multiplexing gain loss. Comparing it to MLSTBC it shows improvement in diversity without deteriorating the rate.

Table 5.1: Rate and Diversity Tradeoff for Various Schemes

Scheme (N, n, N)	d_{max}	r_{max}	D-M trade-off
V-BLAST (Nulling)	1	N	$1 - r/N$
D-BLAST	N	N	$N(1 - r/N)$
MLSTBC	n^2	$K = N/n$	$n^2(1 - r/K)$
TMLSTBC	nN	$K = N/n$	$nN(1 - r/K)$

5.4 Simulation Results

The proposed scheme with parameters $(4, 2, 4)$ is simulated over a quasi-static fading with frame length $L = 100$. Each layer is encoded by a separate rate 1/2 convolutional code with generator polynomials $(171, 133)_{oct}$. The output of the two convolutional encoders are spatially interleaved as described above, and the output of the spatial interleaver is applied to two independent STBC encoders, each employing the Alamouti scheme. Binary phase shift keying (BPSK) is assumed. Soft and hard decision Viterbi decoding are considered.

In Figure 5.5, we plot the BER of the proposed TMLSTBC scheme and the MLSTBC schemes with MMSE-QRD *genie* detection. The *genie* detection implies perfect detection of the previous layers, thus no error propagation is assumed [15]. In the figure we demonstrate the simulation results of the first and second layer (sub-group) detected. We observe from the figure the performance improvement achieved by the proposed scheme over the original MLSTBC scheme. It is observed that the first and second group detected for the TMLSTBC scheme experience the same performance. In addition, we observe that, the performance of the TMLSTBC match that of the MLSTBC second detected sub-group. Thus for this case of a $(4, 2, 4)$ system, we demonstrate that the TMLSTBC scheme achieves a diversity gain of 2×4, as does the MLSTBC second group detected.

In Figure 5.6, we plot the overall simulation results of the proposed TMLSTBC architecture, along with the overall simulation results of the MLSTBC scheme with both the GIC and MMSE-QRD detectors. In the simulation results for this figure we have assumed hard decisions Viterbi decoding. We can observe that the performance results of the proposed TMLSTBC architecture has a great advantage than the MLSTBC architecture. We see a performance gain of 3dB at 10^{-5}.

In Figure 5.7, we plot the overall simulation results of the proposed MLSTBC architecture, along with the overall simulation results of the MLSTBC scheme with both the GIC and MMSE-QRD detectors, but this time we assume soft decision Viterbi decoding and the *genie* detection is applied. We also plot in the same figure theoretical results. The theoretical results follow equation (5.9) with the number of transmit and receive antennas indicated

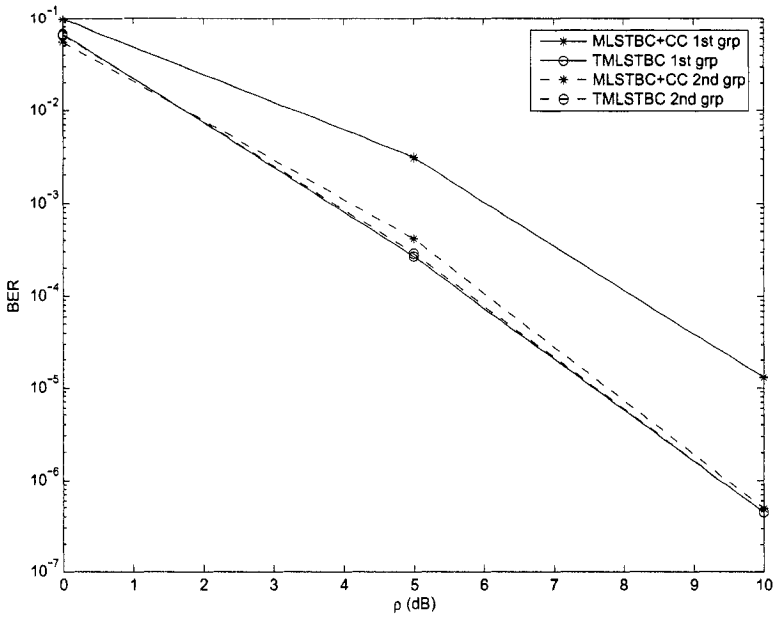

Figure 5.5: BER performance results of the proposed TMLSTBC and MLSTBC schemes with the *genie* detection applied.

in the legend. Thus, once again we see from the simulation results that the TMLSTBC architecture has the same diversity order as a 2×4 MIMO system.

In Figure 5.8, we plot the BER performance of the TMLSTBC and MLSTBC scheme for the overall performance with error propagation at each detection stage, i.e., no *genie* detection. The figure further justifies the performance improvements of the proposed scheme. There is a 3.0 dB gain between the TMLSTBC and MLSTBC at BER 10^{-5} for hard decision Viterbi decoding, and a gain of 3 dB at 10^{-6} for soft decision Viterbi decoding.

In Figure 5.9, we plot the BER performance results of the TMLSTBC with four transmit and three and four receive antennas respectively. Plotted in the same figure, are the simulation results of the STBC scheme with two transmit and three and four receive antennas. From the simulation results presented in the figure. It is evident that the TMLSTBC achieves the same diversity rate as an STBC code with the same number of receive antennas. That is for the $(4, 2, 3)$ TMLSTBC scheme achieves the same diversity of the 2×3 STBC scheme, thus a diversity of 6 is achieved. Moreover, the $(4, 2, 4)$ TMLSTBC scheme achieves the same diversity as a 2×4 STBC scheme, thus a diversity of 8 is achieved.

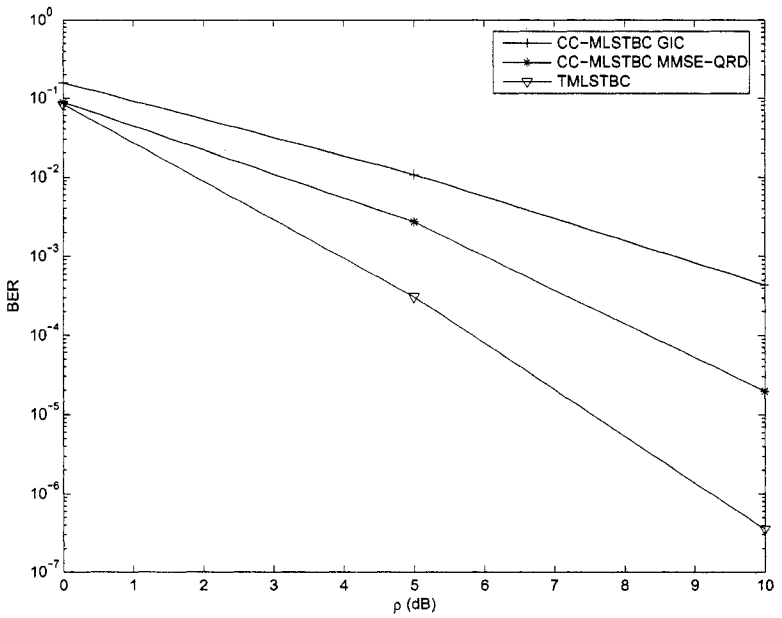

Figure 5.6: BER overall system performance of TMLSTBC and MLSTBC schemes.

5.5 Chapter Summary

In this chapter, we have presented a new transceiver architecture based on concepts from the MLSTC and TSTC schemes in an effort to achieve an enhanced trade-off between the spatial rate and diversity which we call TMLSTBC. The TMLSBC architecture, provides improved performance compared to the MLSTBC without adding complexity to the decoder. The proposed architecture also demonstrates superior trade-off between the diversity and multiplexing gain when comparing it to the original MLSTBC scheme, since the diversity order has increased but the rate has remained the same as in the MLSTBC scheme.

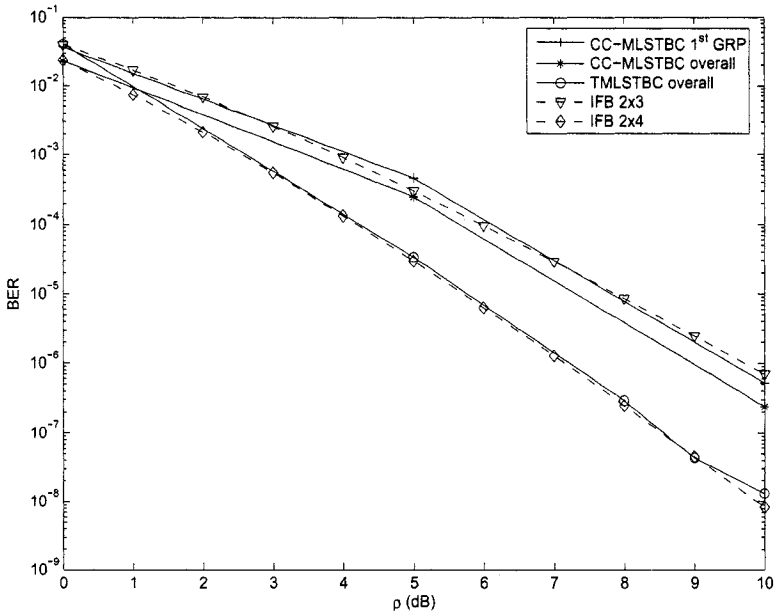

Figure 5.7: BER overall system performance results of the TMLSTBC and MLSTBC schemes with soft decision Viterbi decoding.

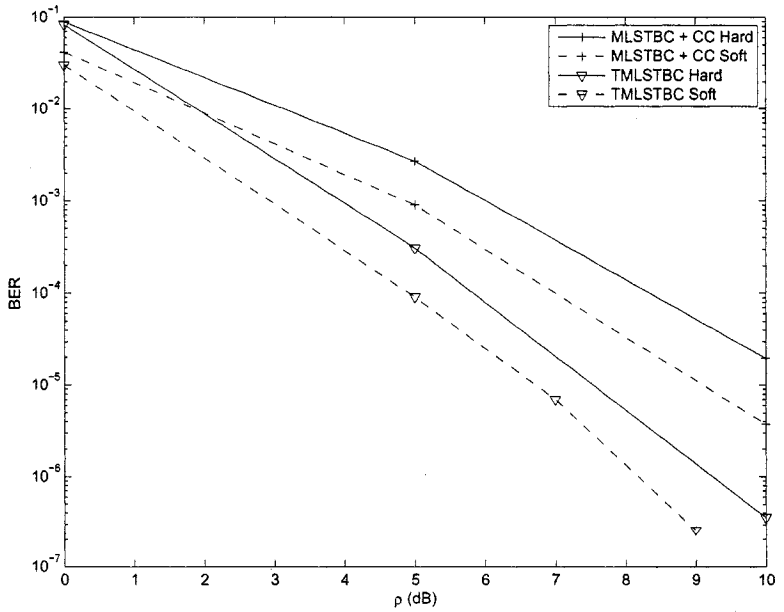

Figure 5.8: BER results of overall system

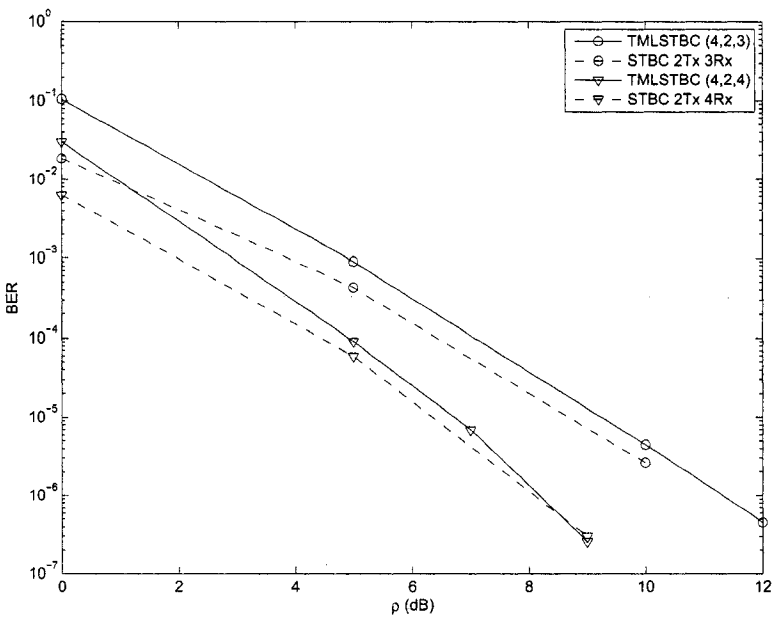

Figure 5.9: BER performance of TMLSTBC scheme with different number of receive antennas.

Chapter 6

Conclusions and Future Work

6.1 Conclusion

In this thesis we focused on finding MIMO systems, which provide the best spatial rate and spatial diversity gain trade-off while maintaining low complexity. The LST codes and STBCs are the best STC schemes in terms of complexity to provide high data rate transmission and diversity gain, respectively. Both schemes take advantage of low complexity linear processing at the receiver. By combining LST and STBC schemes, we can capitulate both gains simultaneously.

Through our analysis, we demonstrated that the performance of the proposed MMSE-QRD detector in conjunction with the MLSTBC architecture increased the diversity gain of the system. It was also demonstrated that added performance was reached with the sorted algorithm (MMSE-SQRD) and that by applying the PA strategy, the performance gap between the different layers of the MLSTBC architecture can be brought closer, which is an important feature for multiuser systems. It was also found that the proposed MMSE-QRD detector has reduced computational complexity compared to the GIC detector previously applied to the MLSTBC architecture. Additionally the MMSE-QRD detector has the advantage of being able to detect with a reduced number of receive antennas.

Furthermore, it was established that by extending the MLSTBC with OFDM, frequency diversity was extracted from the frequency selective channel.

Finally, it was concluded that our proposed transceiver architecture based on concepts from the MLSTC and TSTC schemes, achieves an enhanced trade-off between the spatial rate and diversity.

6.2 Future Work

- In a wideband wireless communication system, there is the existence of a multipath channel. Consequently, ISI is subjected to the received signal. Thus, the next step of our work is to expand the TMLSTBC scheme to a frequency selective channel. In this work we will investigate the diversity order of the scheme, as well as the multiplexing gain.

- A interesting proposition is to apply the TMLSTBC scheme in a cooperative wireless network. A study will be conducted to include the diversity gain and the multiplexing gain available from such a network. If data is to be transmitted from the source **S** in a relay channel, to destination terminal **D**. Due to the broadcast channel, another terminal in the network, which we denote as the relay terminal **R**, also receive the signal from **S** and thus can cooperate with **S** to accomplish the communication with **D**. In this case, the antenna on **S** and that on **R** form a virtual transmit antenna array which realizes spatial diversity gain in a distributed fashion, but the delay between the received signal copies at **D** due to processing delay at **R** need be taken into the consideration for transmit antenna selection this time.

- The GIC decoder can be applied either serially or in parallel. The serial GIC decodes the strongest layer after nulling all other layers and then the contribution of it is canceled from the received signal and the serial nulling and cancellation is repeated fro all other layers. The parallel GIC algorithm consists of two stages. The first is the parallel nulling followed by parallel interference cancellation and detection of all layers. We wish to try different decoding schemes for the MMSE-QRD detector and try different combinations of serial/parallel configurations.

- So far we are assuming perfect channel knowledge at the detector. A separate channel estimator can provide channel knowledge to the detector. Usually the channel estimation is based on the known sequence of bits, which is unique for a certain transmitter and which are repeated in every transmission burst. Thus, the channel estimator is able to estimate the channel impulse response for each burst separately by exploiting the known transmitted bits and the corresponding received samples. We would like to apply the MLSTBC and TMLSTBC schemes with detectors that will require channel estimation. Channel estimation can be accomplished by means of the Least-squares (LS) channel estimation techniques.

Bibliography

[1] I. E. Telatar, "Capacity of multi-antenna Gaussian channels," *European Trans. on Telecommun.*, vol. 10, no. 6, pp. 585–595, Nov.1999.

[2] P. W. Wolniansky, G. J. Foschini, G. D. Golden, and R. A. Valenzuela, "V-BLAST: an architecture for realizing very high data rates over the rich-scattering wireless channel," *Proc. IEEE SSSE-98*, pp.295-300, Sept. 1998.

[3] C. E. Shannon, "The mathematical theory of communication," *Illinoise Press, Urbana Illinois,* 1959.

[4] G. J. Foschini, "Layered space-time architecture for wireless communication in a fading environment when using multi-element antennas," *Bell Labs Technical Journal,* vol. 1, no. 2, Autumn 1996.

[5] V. Tarokh, N. Seshadri and A.R. Calderbank, "Space-time codes for high data rates wireless communications: performance criterion and code construction," *IEEE Trans. on Inf. Theory*, vol. 44, no. 2, pp. 744-765, Mar. 1998.

[6] S. Alamouti, "A simple transmit diversity technique for wireless communication," *IEEE J. Select. Areas Commun.* vol. 16, no. 8, pp. 1451-1458, Oct. 1998.

[7] V. Tarokh, H. Jafarkhani, and A. R. Calderbank, "Space-time block codes from orthogonal designs," *IEEE Trans. On Inf. Theory*, vol. 45, no. 5, July 1999.

[8] G. Foschini and M. Gans, "On the limits of wireless communication in a fading environment when using multiple antenna," *Wireless Personal Comm.* vol. 6, no. 3, pp. 311-335, March 1998.

[9] L. Zheng and D. Tse, "Diversity and multiplexing: a fundamental tradeoff in multiple-antenna channels," *IEEE Trans. Inf. Theory,* vol. 49, no. 5, pp. 1073-1094, May 2003.

[10] A.R. Calderbank, A. F. Naguib, and N. Seshadri, "Applications of space-time block codes and interference suppression for high capacity and high data rate wireless systems," *IEEE ACSSC*, vol. 2, pp. 1803-1810, Nov. 1998.

[11] R. Calderbank, H. Jafarkhani, and V. Tarokh, "Space-time block coding for wireless communications: performance results," *IEEE Selected Areas in Comm.*, vol. 17, no. 3, pp. 451-460, March 1999.

[12] G.D. Golden, C.J. Foschini, R.A. Valenzuela, and P.W. Wolniansky, "Detection algorithm and initial laboratory results using V-BLAST space-time communication architecture," *Electronics Letters*, vol. 35, Iss. 1, pp.14 – 16, Jan. 1999.

[13] D. Shiu and J. M. Kahn, "Layered space-time codes for wireless communications using multiple transmit antennas," *IEEE Intl. Conf. on Commun.*, pp. 436-440, June 1999.

[14] G. Foschini, G. Golden, R. Valenzuela, and P. Wolniansky. "Simplified processing for high spectral efficiency wireless communication employing multi-element arrays," *IEEE Journal on Selected Areas in Commun.*, vol. 17, no. 11, Nov. 1999.

[15] R. Buhnke, D. Wubben, V. Kuhn and K. D. Kameyer, "Efficient algorithm for detecting layered space-time codes," *4th ITG Conf. on Source and Channel Coding*, 2002.

[16] F. Gagnon, and S. Loyka, "Performance analysis of the V-BLAST algorithm: an analytical approach," *International ETH Seminar on Broadband Commun.*, Feb. 2002.

[17] F. Gagnon, and S. Loyka, "Analytical framework for outage and BER analysis of the V-BLAST algorithm," *IEEE Seminar on Commun.*, pp. 120 – 123, Feb, 2004.

[18] Y. Jiang, J. Li, and X. Zheng, "Asymptotic performance analysis of V-BLAST," *IEEE Globecom Conf.*, vol. 6, pp. 3882-3886, Nov. 2005.

[19] B. Vucetic and J. Yuan, *Space-Time Coding*, Wiley, 2003.

[20] V. Tarokh, A. Naguib, N. Seshadri, and A.R. Calderbank, "Combined array processing and space-time coding," *IEEE Trans. Inf. Theory*, vol. 45, no. 4, pp. 1121-1128, May 1999.

[21] T. Mao, and M. Motani, "STBC-VBLAST for MIMO wireless communication systems," *IEEE International Conf. on Commun.*, vol. 4, pp. 2266 – 2270, May 2005.

[22] P. H. W. Fung, S. Sun, and T. T. Tjhung, "Soft decision-based iterative interference cancellation (IIC) in group-wise STBC (G-STBC) MIMO systems," *IEEE Vehciular Techno. Conf.*, vol. 2, pp. 984-988, April 2003.

[23] J. G. Proakis, *Digital Communications,* 4th Ed., McGraw Hill, 2000.

[24] R. Buhnke, D. Wubben, V. Kuhn and K. D. Kameyer, "MMSE extension of V-BLAST based on sorted QR decomposition," *IEEE Vehciular Techno. Conf.*, vol. 1, pp. 508-512, Oct. 2003.

[25] R. Bohnke, V. Kuhn, K. D. Kammeyer, and D. Wubben, "Reduced Complexity MMSE Detection for BLAST architectures," *IEEE Globecomm Conf.,* vol. 4, pp. 2258-2262, Dec. 2003.

[26] K. B. Lee, and S. H. Nam, "Transmit power allocation for an extended V-BLAST system," *IEEE, 13th International Symposium on Radio Commun.*, vol.2, pp.843-848, Sept. 2002.

[27] K. Bok, S. H. Nam, and O. Shin, "Transmit power allocation for a modified V-BLAST system," *IEEE Transactions on Commun.*, vol. 52, iss. 7, pp. 1074-1079, July 2004.

[28] Y. Li, and G. L. Stuber, *Orthogonal Frequency Division Multiplexing for Wireless Communications*, Springer-Verlag, 2005.

[29] D. Agrawal, A. Naguib, V. Tarokh, and N. Seshadri, "Space-time coded OFDM for high data-rate wireless communication over wideband channels," *IEEE Vehciular Techno. Conf.*, vol. 3, pp. 2232-2236, May 1998.

[30] E. Larson, *Space-Time Block Coding for Wireless Communications,* Cambridge University Press, 2003.

[31] H. Jafarkhani *Space-Time Coding*, Cambridge University Press, 2005.

[32] L. Lin, L.J. Cimini, and J.C. Chuang, "Comparison of convolutional and turbo codes for OFDM with antenna diversity in high-bit-rate wireless applications," *IEEE Commun. Letters*, vol. 4, no. 9, pp. 277-279, Sept. 2000.

[33] R.Prasad *OFDM for Wireless Communication Systems*, Artech House, 2004.

[34] A. Paulraj, R. Nabar, and D. Gore, *Introduction to Space-Time Wireless Communication*, Cambridge University Press, 2003.

[35] J. Heiskala, J. Terry, *OFDM Wireless LANS: A Theoretical and Practical Guide*, SAMS, 2002.

[36] L. Litwin, and M. Pugel, "The principles of OFDM," www.rfdesign.com, Jan. 2001.

[37] Z. Lei, S. Sun, and W. Yan, "A low complexity V-BLAST OFDM detection algorithm for wireless LAN systems," *IEEE Commun. Letters*, vol. 8, iss. 6, pp. 374-376, Jun. 2004.

[38] B. Gui, and D. Qu, "VBLAST-OFDM system with linear constellation precoding," *IEEE Vehciular Techno. Conf.*, vol.2, pp. 733-737, May 2004.

[39] S. Sun, Y. Li, T. T. Tjhung, and Y. Wu, "A novel iterative receiver for coded MIMO OFDM systems," *IEEE International Conf. on Commun.*, vol. 4, pp. 2473-2477, June 2004.

[40] A Ibrahim, and M. Khairy, "Multilayered space-time block codes for OFDM systems," *IEEE International Conf. on Elect. and Comp. Eng.*, Sept. 2004.

[41] R. Buehrer, S. Al-Ghadhban, M. Mohammad, and B. Woerner, "Performance evaluation of decoding algorithms for multi-layered STBC-OFDM systems," *IEEE Asilomar Conf. on Signal Systems and Comp.*, vol. 1, pp. 1208 – 1212, Nov. 2004.

[42] Ben Lu and X. Wang, "Space-time code design in OFDM systems," *IEEE GLOBECOM Conf.*, vol. 2, pp. 1000 – 1004, Dec. 2000.

[43] Y. Gong, and K. Letaief, "Space-frequency-time coded OFDM for broadband wireless communications," *IEEE Globecom Conf.*, pp. 519-523, Nov. 2001.

[44] Y. Gong, and K. B. Letaief, "An efficient space-frequency coded OFDM system for broadband wireless communications," *IEEE Transactions on Commun.*, vol. 51, no. 11, pp. 2019 – 2029, Nov. 2003.

[45] El Gamal, H.Hammons, L. Youjian, M. P. Fitz, and O. Y. Takeshita, "On the design of space-time and space-frequency codes for MIMO frequency-selective fading channels," *IEEE Trans. Inf. Theory*, vol. 49, no. 9, pp. 2277- 2292, Sept. 2003.

[46] Richard C. Singleton, "Maximum distance q-nary codes," *IEEE Transactions on Inf. Theory*, vol.10, no.2, pp.116–118, April 1964.

[47] H. El Gamal and A. R. Hammons, "A new approach to layered space-time coding and signal processing," *IEEE Trans. Inf. Theory,* vol. 47, no. 6, pp. 2321-2334, Sept. 2001.

[48] D. Tse and P. Viswanath, *Fundamentals of Wireless Communication*, Cambridge University Press, 2005.

[49] C. Fangjiong, W. Gang, and L. Xiaowei, "A joint detection method for horizontal-BLAST architecture," *IEEE International Symposium on Wireless Commun.,* vol. 2, pp. 987-990, Aug. 2005.

[50] S. G. Glisic, *Advanced Wireless Communications,* Wiley, 2004.

[51] M. Jankiraman, *Space-Time Codes and MIMO Systems*, Artech House, 2004.

[52] T. Duman and A. Ghrayeb, *Coding for MIMO Communication Systems*, John Wiley and Sons, 2007.